Australian Government
Department of Defence
Defence Science and
Technology Organisation

Data Reduction Algorithms for Store Separation Grid Testing

Jonathan Dansie and Adam Blandford

Aerospace Division
Defence Science and Technology Organisation

DSTO-TN-1339

ABSTRACT

Store separation testing is undertaken to ensure that stores can be safely released from aircraft in flight. Grid testing in wind tunnels produces data that can be used to predict store separation behaviour. This document describes the algorithms used to prepare test plans for store separation grid testing and to reduce grid data to the form required for analysis. The information is presented in a general form, and may also provide a useful reference for other forms of wind tunnel testing.

RELEASE LIMITATION

Approved for public release

Published by

Aerospace Division
DSTO Defence Science and Technology Organisation
506 Lorimer St
Fishermans Bend, Victoria 3207 Australia

Telephone: 1300 DEFENCE (1300 333 363)
Fax: (03) 9626 7999

AR-016-054
August 2014

APPROVED FOR PUBLIC RELEASE

Data Reduction Algorithms for Store Separation Grid Testing

Executive Summary

The release of stores from an aircraft, including fuel tanks and ordnance, poses a risk that must be managed in order to safely employ stores during operations. Under some conditions, particularly at high-speed, the store may make unintended contact with the aircraft, endangering the lives of personnel and causing equipment damage. Management of the risk involves ground and flight testing to understand the behaviour of stores during separation from the aircraft. Wind tunnel testing is an integral part of stores clearance projects.

The Defence Science and Technology Organisation (DSTO) has an integral role in supporting Royal Australian Air Force (RAAF) stores clearance campaigns through wind tunnel testing and store trajectory prediction. Store separation tests for modern fighter aircraft are undertaken in the DSTO transonic wind tunnel. DSTO uses a grid technique, where aerodynamic data are gathered in a prescribed grid pattern below the store carriage position. This grid covers the region that the store is expected to travel through after release from its parent aircraft. The aerodynamic data is then combined with other information, including mass and moments of inertia of the store, to predict the store's trajectory following release from the aircraft.

The algorithms required to prepare a test plan for a transonic wind tunnel grid test are described in this document. Also included are the processes used to reduce wind tunnel grid data to the form required for analysis of store release trajectories. The implementation of these algorithms for specific applications is not discussed, but examples are provided to aid with development and validation of software. The algorithms are presented in a general form and this document may provide a useful reference for other forms of wind tunnel testing.

This page is intentionally blank

Contents

Figures

Notation

Abbreviations and Acronyms

AIAA	American Institute of Aeronautics and Astronautics
AOSG	Air Operations Support Group
ASC	Aircraft-Stores Compatibility
BMC	Balance Moment Centre
c.g.	Centre of gravity
DSTO	Defence Science and Technology Organisation
DSTOres	Defence Science and Technology Organisation release evaluation suite
LDT	Linear Displacement Transducer
MATLAB	MATrix LABoratory
MRC	Model Moment Reference Centre
RAAF	Royal Australian Air Force
SS	Store Support
STEME	Store Trajectory Estimation in a MATLAB Environment
TWT	Transonic Wind Tunnel

Angles

$\phi_{c,b}$, $\theta_{c,b}$, $\psi_{c,b}$	Roll, pitch and yaw angles of the store body axes relative to carriage axes.
$\phi_{ac,c}$, $\theta_{ac,c}$, $\psi_{ac,c}$	Roll, pitch and yaw angles of the carriage axes relative to aircraft axes.
$\phi_{g,ac}$, $\theta_{g,ac}$, $\psi_{g,ac}$	Roll, pitch and yaw angles of the aircraft axes relative to tunnel axes.
$\phi_{g,b}$, $\theta_{g,b}$, $\psi_{g,b}$	Roll, pitch and yaw angles of the store body axes relative to tunnel axes.
$\phi_{g,ss}$, $\theta_{g,ss}$, $\psi_{g,ss}$	Roll, pitch and yaw angles calculated from feedback of the store support arm sensors.
ξ_1, ξ_2, ξ_3	Angular misalignment between balance and store body axes, defined in Appendix B.1.
α, β	Incidence (tangent definition) and sideslip (sine definition) orientation angles, relative to the wind direction. In the absence of flow angularity corrections this corresponds to the tunnel gravity axes.

Displacements

$x_{c,b}$, $y_{c,b}$, $z_{c,b}$	Displacement of the store in carriage axes.
$x_{g,b}$, $y_{g,b}$, $z_{g,b}$	Displacement of the store in tunnel axes, relative to carriage position.
x_g, y_g, z_g	Displacement of the store in tunnel axes, relative to tunnel reference point.
$x_{g,c}$, $y_{g,c}$, $z_{g,c}$	Displacement of the carriage position in tunnel axes.
$x_{g,ss}$, $y_{g,ss}$, $z_{g,ss}$	Displacement calculated from feedback of the store support sensors.
x_b, y_b, z_b	Displacement of the model moment reference centre relative to the

balance moment centre in balance axes.

x_{cg}, y_{cg}, z_{cg} Displacement of the real store centre of gravity with respect to the model reference point, in store body axes.

Forces and Moments

$$\boldsymbol{H_T} = \begin{bmatrix} F_{BALT} \\ M_{BALT} \end{bmatrix} = \begin{bmatrix} F_{XBALT} \\ F_{YBALT} \\ F_{ZBALT} \\ M_{XBALT} \\ M_{YBALT} \\ M_{ZBALT} \end{bmatrix}$$

Tare loads in balance axes.

$$\boldsymbol{H_G} = \begin{bmatrix} F_{BALG} \\ M_{BALG} \end{bmatrix} = \begin{bmatrix} F_{XBALG} \\ F_{YBALG} \\ F_{ZBALG} \\ M_{XBALG} \\ M_{YBALG} \\ M_{ZBALG} \end{bmatrix}$$

Gross loads in balance axes.

$$\boldsymbol{H} = \begin{bmatrix} F_{BAL} \\ M_{BAL} \end{bmatrix} = \begin{bmatrix} F_{XBAL} \\ F_{YBAL} \\ F_{ZBAL} \\ M_{XBAL} \\ M_{YBAL} \\ M_{ZBAL} \end{bmatrix}$$

Aerodynamic loads in balance axes.

$$\boldsymbol{F} = \begin{bmatrix} F_X \\ F_Y \\ F_Z \end{bmatrix}, \quad \boldsymbol{M} = \begin{bmatrix} M_X \\ M_Y \\ M_Z \end{bmatrix}$$

Aerodynamic loads (forces and moments) in store body axes.

$$\boldsymbol{F_{c.g.}} = \begin{bmatrix} F_{Xc.g.} \\ F_{Yc.g.} \\ F_{Zc.g.} \end{bmatrix}, \quad \boldsymbol{M_{c.g.}} = \begin{bmatrix} M_{Xc.g.} \\ M_{Yc.g.} \\ M_{Zc.g.} \end{bmatrix}$$

Aerodynamic loads (forces and moments) about the real store centre of gravity.

Aerodynamic Force and Moment Coefficients

C_X, C_Y, C_Z Axial, lateral and normal force coefficients in store body axes.
C_l, C_m, C_n Rolling, pitching and yawing moment coefficients in store body axes.

Strain Gauge Balance Parameters

$\boldsymbol{R}$	Vector of absolute strain gauge balance output.
R_i	Component i of strain gauge balance output.
$\boldsymbol{R_0}$	Buoyant zero strain gauge balance output.
$\boldsymbol{R'_0}$	Wind-off zero strain gauge balance output.
$\boldsymbol{R_T}$	Tare load strain gauge balance output.
$\boldsymbol{R'}$	Wind-on strain gauge balance output.
$[C1]$	Linear calibration coefficients.
$[C2]$	Non-linear calibration coefficients.
$\boldsymbol{H}$	Vector of measured loads.
$\boldsymbol{H^*}$	Vector of squares and cross products of component loads.
k_X, k_Y, k_Z, k_{MX1}, k_{MX2}, k_{MY1}, k_{MY2}, k_{MZ1}, k_{MZ2}	Tare weight coefficients.
$\boldsymbol{K}$	Matrix of sting-balance deflection coefficients.
$k_1, k_2, \ldots, k_{10}$	Sting-balance deflection coefficients.
x', y', z'	Axial, lateral and normal deflections in balance axes.
ν, η, χ	Roll, pitch and yaw angular deflections in balance axes.

Transformation Matrices

$M_{c,b}$	Euler rotation matrix from store axes to carriage axes.
$M_{ac,c}$	Euler rotation matrix from carriage axes to aircraft axes.
$M_{g,ac}$	Euler rotation matrix from aircraft axes to tunnel axes.
$M_{g,c}$	Euler rotation matrix from carriage axes to tunnel axes
$M_{g,b}$	Euler rotation matrix from store axes to tunnel axes.
$M_{g,ss}$	Euler rotation matrix from store support arm to tunnel axes.
$M_{ss,b}$	Pseudo-Euler rotation matrix from store support arm to store body axes.
$M_{b,bal}$	Non-Euler rotation matrix from balance axes to store body axes.
$M_{w,b}$	Euler rotation matrix from store body axes to wind axes.
$M_{p,b}$	Euler rotation matrix from store body axes to missile axes.

Wind Tunnel Parameters

M	Freestream Mach number.
q	Freestream dynamic pressure.
P_t	Tunnel total pressure.
P_s	Tunnel static pressure.
Re	Reynolds number.
γ	Ratio of specific heats.
ρ	Freestream density.
R	Gas constant.
T_s	Tunnel static temperature.
μ	Freestream kinematic viscosity.

$\boldsymbol{V}$	Freestream velocity vector
u, v, w	Components of freestream velocity in tunnel axes.

Model Parameters

d	Model reference dimension.
S	Model reference area.

1. Introduction

When stores are released from an aircraft they may encounter a highly non-uniform flow field produced by the parent aircraft, particularly at high speeds. Stores include any removable object that may be attached to an aircraft, and which can be released during flight. This includes fuel tanks, avionic and storage pods, missiles, bombs, pylons and racks. The aerodynamic interaction between the store and the parent aircraft may lead to contact between the store and the aircraft, endangering the lives of personnel and causing severe equipment damage. For this reason, it is important to predict the separation behaviour of stores to ensure they can be safely employed in-flight. The Air Operations Support Group (AOSG) is the responsible agency for ensuring that the weapon is safe to carry and release from Royal Australian Air Force (RAAF) aircraft. Australia uses an approach based on the methodology of MIL-HDBK-1763 [1] for certification of aircraft-stores compatibility (ASC) and flight clearances.

Assessment of employment and jettison characteristics for ASC is one element of the MIL-HDBK-1763 methodology. For this assessment, the Defence Science and Technology Organisation (DSTO) and AOSG use a 'grid method' [2] whereby an aerodynamic force and moment database is generated by testing a model of the store in a wind tunnel facility with a model of the parent aircraft. The store model, mounted on a six degree-of-freedom support arm via an internal strain gauge balance, is positioned at pre-defined grid points in the region where the store is expected to travel when it is released. Aerodynamic forces and moments are measured at each grid point for a range of store attitudes. These forces and moments are then used in a trajectory prediction computer program together with a database of the freestream aerodynamics of the store in isolation and a variety of other inputs including store mass and moments of inertia data, ejector force and distribution models and atmospheric properties. DSTO uses an in-house developed program, DSTO release evaluation suite (DSTOres), for trajectory prediction, and AOSG use their own prediction program, Store Trajectory Estimation in a MATLAB Environment (STEME) [3].

Wind tunnel testing for store release at DSTO is conducted in the DSTO Transonic Wind Tunnel (see Appendix A for basic information on this facility). A sub-scale model of the store is mounted on a six degree-of-freedom actuated support. This support system allows the store to be rotated at varying roll, pitch and yaw angles and translated axially, laterally and vertically within a three-dimensional plane. A sub-scale half-model of the parent aircraft is mounted to a turntable support on the tunnel test section sidewall enabling a pitch rotation. The validity of this method has been verified in a number of store separation tests [4]. The store is positioned at pre-defined grid points in the region it is expected to travel through after release from the parent aircraft. Aerodynamic forces and moments are measured at each grid point, for a variety of store orientations, by a strain-gauge balance that is integral to the support arm.

This document describes the algorithms required to prepare transonic wind tunnel grid test plans and to reduce wind tunnel grid data to the form required for input into store trajectory prediction software. Sections 2 and 3 provide the definitions of axis systems and angles, respectively, used during aerodynamic testing at DSTO. Section 4 describes the

transformations between coordinate systems and the process of defining the store grid for testing. Section 5 outlines the process for reducing measured strain gauge balance data into the aerodynamic forces and moments required for store release prediction. Example calculations for both test preparation and data reduction are presented in Appendix C, and can be used to validate software implementations of the data reduction algorithms presented in this report.

2. Definition of Axis Systems

The following axis systems are used in this document. These axis system definitions generally conform to the AIAA Guide *Nomenclature and Axis Systems for Aerodynamic Wind Tunnel Testing* [5].

2.1 Tunnel Gravity Axis System

The gravity axis system is an Earth fixed axis system, which has its z-direction aligned with the gravity vector. The origin is located at the nominal centre of the test section, which corresponds to the centre of the sidewall turntable, and is 400 mm laterally from the inner sidewall. It is defined as station 5257 in [6, §2.1.2.2]. The axes are shown in Figure 1 and are defined as follows:

X_g Gravity longitudinal axis, perpendicular to the gravity vector and contained in a plane parallel to the support system pitch plane, positive upstream.

Y_g Gravity lateral axis, perpendicular to the gravity X_g-Z_g plane, positive direction determined by the positive X_g and Z_g directions in conjunction with the right-hand rule.

Z_g Gravity vertical axis, collinear with the gravity vector, positive toward the tunnel floor.

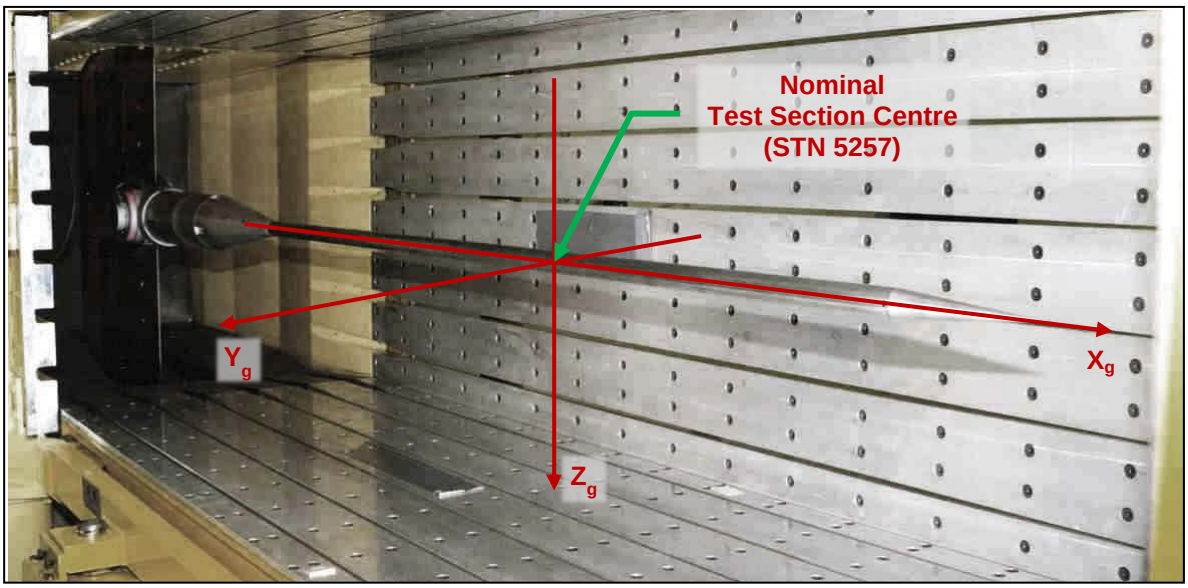

Figure 1 Tunnel gravity axis system

2.2 Balance Axis System

The balance axis system origin is fixed at the balance moment centre (BMC) about which forces and moments were resolved during calibration. This is defined as the geometric centre of the gauged elements as shown in Figure 2.

The X_{bal}, Y_{bal}, and Z_{bal} coordinate axes rotate with the strain gauge balance and are defined as follows:

X_{bal} Collinear with the strain gauge balance longitudinal axis, positive towards the metric end.

Y_{bal} Perpendicular to the strain gauge balance X_{bal}-Z_{bal} plane, positive direction determined by the positive X_{bal} and Z_{bal} directions in conjunction with the right-hand rule.

Z_{bal} Collinear with the gravity axis when the strain gauge balance is orientated with zero pitch and roll, positive downwards.

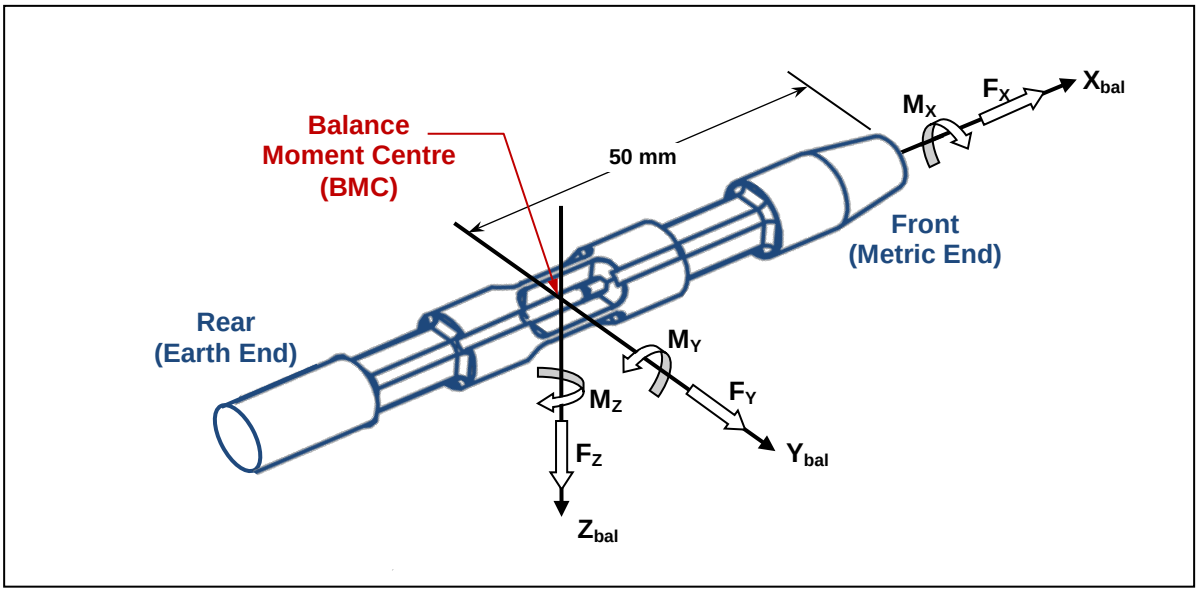

Figure 2 Balance axis system (DSTO-BAL-08 shown)

2.3 Store support axis system

The store support axis system defines the position and orientation measured by the store support system encoders. The origin of the store support axis system is located at a fixed distance from the store support pitch pivot point along the store support x axis, as shown in Figure 3. This distance represents the chosen centre of orientation for the model, which may or may not be coincident with the model reference centre or balance moment centre. Measurements in the store support axis system are uncorrected for balance-sting deflection. The axes X_{ss}, Y_{ss} and Z_{ss} are defined as follows:

X_{ss} Store support longitudinal reference axis, positive upstream.

Y_{ss} Perpendicular to the store support X_{ss}-Z_{ss} plane, positive direction determined by the positive X_{ss} and Z_{ss} directions in conjunction with the right-hand rule.

Z_{ss} Store support vertical reference axis, collinear with the gravity axis when the store support is orientated with zero pitch and roll, positive downwards.

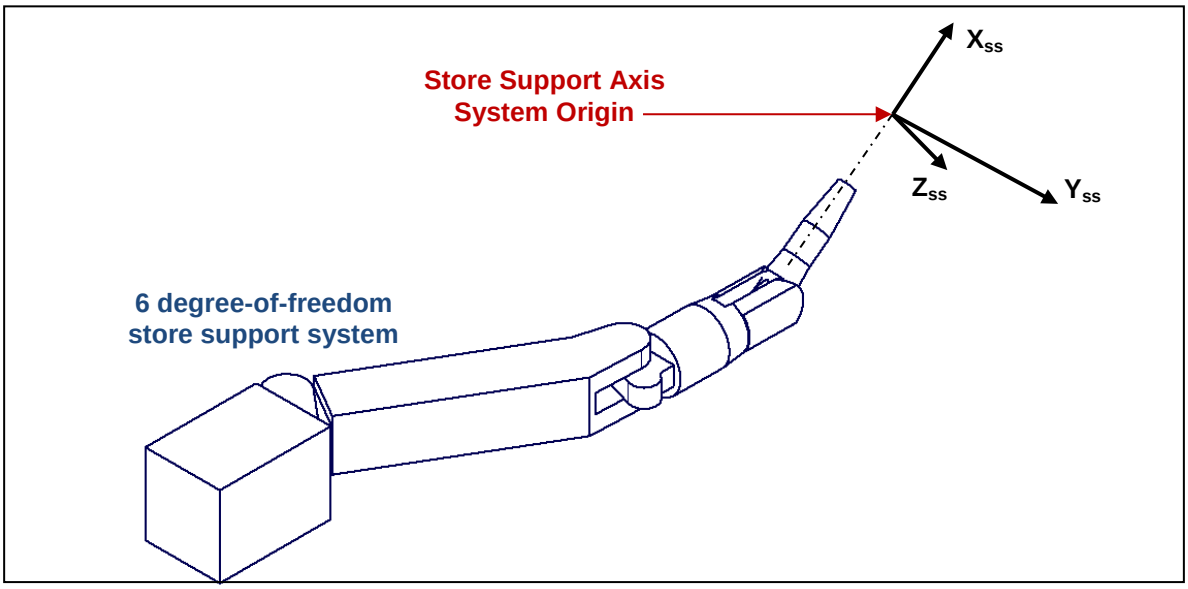

Figure 3 Store support axis system

2.4 Aircraft Axis System

The aircraft axis system is a body axis system which has its origin at the aircraft reference point. The aircraft axis system is shown in Figure 4. Only the directions of the axes are required, and these are defined as follows:

X_{ac} Aircraft longitudinal reference axis, positive toward the nose of the aircraft.

Y_{ac} Aircraft lateral reference axis, perpendicular to the aircraft X_{ac}-Z_{ac} plane and positive as defined by a right-handed system.

Z_{ac} Aircraft vertical reference axis, parallel to and in the same direction as the gravity Z_g axis when the aircraft is upright and level in pitch and roll.

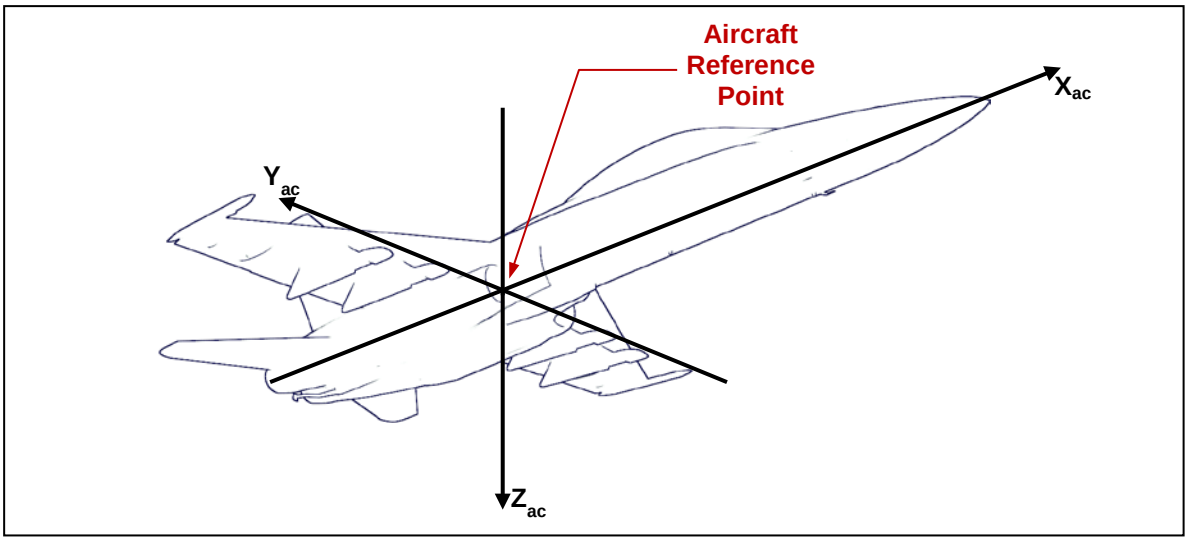

Figure 4 Aircraft axis system

2.5 Store Body Axis System

The store body axis system origin is designated as the model moment reference centre (MRC), as shown in Figure 5. The axes X_b, Y_b, and Z_b are defined as follows:

X_b Model longitudinal reference axis, positive toward the nose of model.

Y_b Model lateral reference axis, perpendicular to the body X_b-Z_b plane and positive as defined by a right-handed system.

Z_b Model vertical reference axis, parallel to and in the same direction as the gravity Z_g axis when the model is upright and level in pitch and roll.

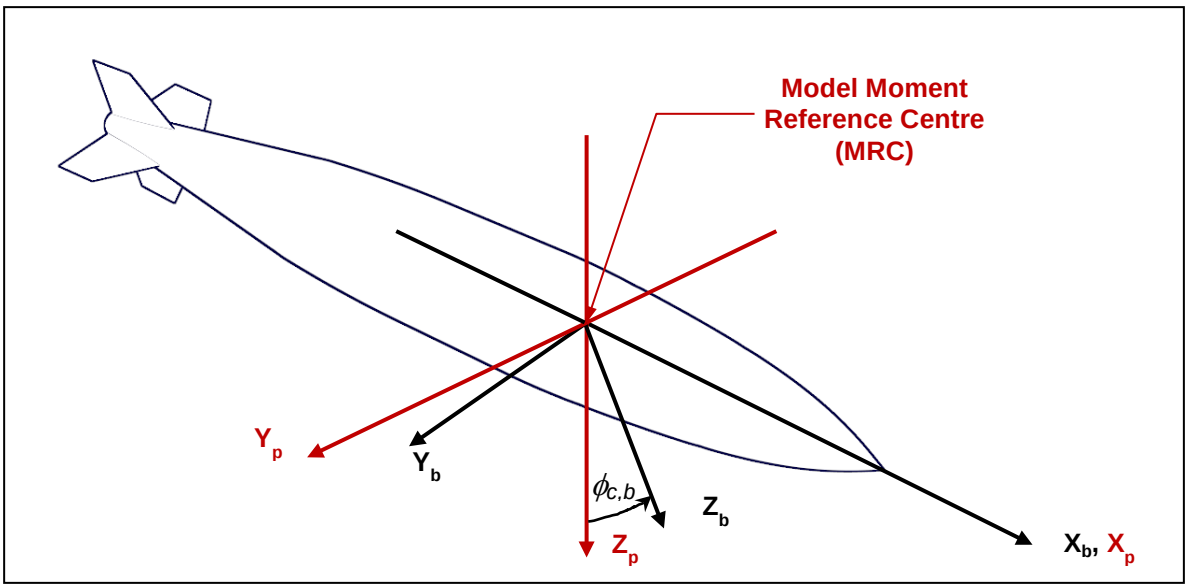

Figure 5 Body axis system, in black, and missile axis system, in red

2.6 Wind Axis System

The origin of the wind axis system is coincident with the body axis system origin at the MRC. The axes X_w, Y_w and Z_w are defined as follows:

X_w Wind longitudinal axis, parallel to the total velocity vector, differs from body X_b axis by the angles α and β.

Y_w Wind lateral axis, perpendicular to the wind X_w axis and contained in the X_w-Y_b plane. Differs from the body Y_b axis by the angle β.

Z_w Wind vertical axis, perpendicular to the to the wind/body axis X_w-Y_b plane and contained in the body axis X_b-Z_b plane. Differs from the body Z_b axis by the angle α.

2.7 Missile Axis System

The origin of the missile axis system is coincident with the body axis system origin at the MRC. The missile axis system rotates with the model through yaw and pitch rotations only. The Y_p axis is coincident with the Y_b axis with the store at zero roll angle (ϕ_{CS}). This feature has led to the missile axis system being called the non-rolling body axis system. The axes X_p, Y_p, and Z_p are shown in Figure 5, and are defined as follows:

X_p Missile longitudinal axis, coincident with and in the same direction as the body X_b axis.

Y_p Missile lateral axis, perpendicular to the missile axis X_p-Z_p plane and positive as defined by a right-handed system.

Z_p Missile vertical axis, perpendicular to the body X_b axis and contained in the (missile axis) pitch plane defined by the body X_b axis and an intersecting gravity vector.

2.8 Carriage Axis System

The origin of the carriage axis system is coincident with the store MRC when the store is positioned at carriage, as illustrated in Figure 6. The origin is fixed with respect to the parent aircraft.

X_c Carriage longitudinal axis, collinear with and in the same direction as the model X_b axis when the store is positioned at carriage.

Y_c Carriage lateral reference axis, perpendicular to the carriage X_c-Z_c plane and positive as defined by a right-handed system.

Z_c Parallel to the carriage ejector stroke direction, positive in the direction of the stroke.

Positions within the carriage axis system are often defined in polar coordinates using the following parameters:

r	Location of the store relative to carriage axes as a radial distance from the store release point in the Y_C-Z_C plane, as shown in Figure 6.
r/D (Calibre)	*r* normalised by store diameter, *D*.
Φ_P (Polar Angle)	Location of the store relative to ejector axes as an angle away from Z_C in the Y_C-Z_C plane. Positive towards positive Y_C axis, as shown in Figure 6. (Note: this is opposite to the right hand rule about X_C.)

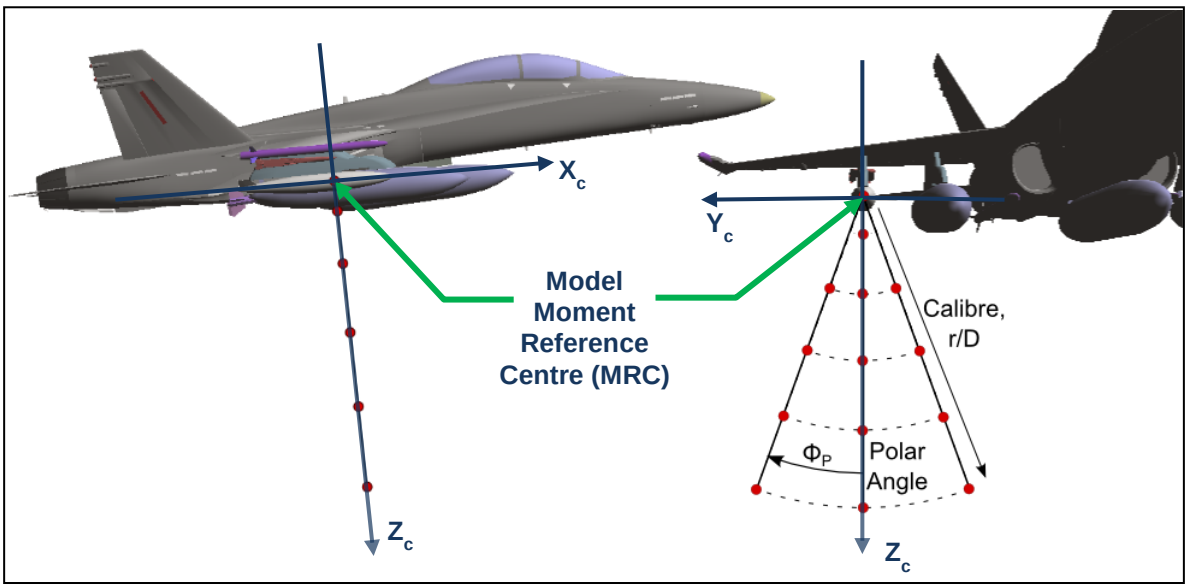

Figure 6 Carriage axis system

3. Definition of Angles

The following definitions of aerodynamic and orientation angles are used for aerodynamic testing at DSTO, including tests performed in the transonic wind tunnel.

3.1 Aerodynamic Angles

Testing in the DSTO wind tunnels uses the tangent definition for incidence and the sine definition for sideslip. Incidence is defined as the angle between the X_b axis and the projection of the wind vector on the X_b-Z_b plane,

$$\tan\alpha = \frac{w}{u} \tag{1}$$

Sideslip is the angle between the wind vector, $\boldsymbol{V}$, and its projection on the model X_b-Z_b plane, v,

$$\sin\beta = \frac{v}{|V|} \tag{2}$$

These angles are limited to the ranges

$$\begin{aligned} -\pi < \alpha \le \pi \\ -\pi < \beta \le \pi \end{aligned} \tag{3}$$

3.2 Orientation Angles

The orientation of one set of axes relative to another is commonly represented by Euler angles. Testing in the DSTO wind tunnels uses the standard yaw (ψ) pitch (θ) and roll (ϕ) angles, applied in the order (ψ, θ, ϕ). To avoid ambiguity, the angles are limited to the following ranges:

$$\begin{aligned} -\pi < \psi \le \pi \\ -\frac{\pi}{2} \le \theta \le \frac{\pi}{2} \\ -\pi < \phi \le \pi \end{aligned} \tag{4}$$

3.3 Transformation between Aerodynamic and Orientation Angles

The aerodynamic angles describe the orientation of the store body axes relative to the tunnel flow axes. In the absence of flow angularity corrections, tunnel flow axes are coincident with tunnel gravity axes. This orientation can also be described by the orientation angles ($\phi_{g,b}$, $\theta_{g,b}$, $\psi_{g,b}$). These two sets of angles are related as follows:

$$\begin{aligned} \tan\alpha &= \tan\theta_{g,b}\cos\phi_{g,b} + \frac{\tan\psi_{g,b}\sin\phi_{g,b}}{\cos\theta_{g,b}} \\ \sin\beta &= \cos\psi_{g,b}\sin\theta_{g,b}\sin\phi_{g,b} - \sin\psi_{g,b}\cos\phi_{g,b} \end{aligned} \tag{5}$$

4. Calculations of Grid Positions

Points within the grid, and store orientations at those points, are defined with respect to the carriage axis system. These points are required in the tunnel axis system during testing, and can be converted using the transforms below.

4.1 Transformations between Reference Frames

A given frame, $\boldsymbol{F_B}$, is related to another frame, $\boldsymbol{F_V}$, by three Euler angles: ψ (yaw), θ (pitch) and ϕ (roll). To transform $\boldsymbol{F_V}$ to $\boldsymbol{F_B}$, these rotations are applied in the order (ψ, θ, ϕ), and to transform $\boldsymbol{F_B}$ to $\boldsymbol{F_V}$ the rotations are applied in the opposite direction and in reverse order, ($-\phi$, $-\theta$, $-\psi$). The transformation from $\boldsymbol{F_B}$ to $\boldsymbol{F_V}$ can be expressed using the equation

$$\boldsymbol{F_V} = M_{V,B}\boldsymbol{F_B} \tag{6}$$

where the transformation matrix $M_{V,B}$, representing the rotations ($-\phi$, $-\theta$, $-\psi$), is [7]:

$$\begin{aligned} M_{V,B} &= M_3(-\psi).M_2(-\theta).M_1(-\phi) = M_{B,V}^T \\ &= \begin{bmatrix} \cos\theta\cos\psi & \sin\phi\sin\theta\cos\psi - \cos\phi\sin\psi & \cos\phi\sin\theta\cos\psi + \sin\phi\sin\psi \\ \cos\theta\sin\psi & \sin\phi\sin\theta\sin\psi + \cos\phi\cos\psi & \cos\phi\sin\theta\sin\psi - \sin\phi\cos\psi \\ -\sin\theta & \sin\phi\cos\theta & \cos\phi\cos\theta \end{bmatrix} \end{aligned} \tag{7}$$

The following rotation matrices are required for transformation to and from grid points. Each matrix can be determined by substituting the appropriate angles into Equation 7.

$M_{c,b}$ = Transformation from store axes to carriage axes
– order of rotations ($-\phi_{c,b}$, $-\theta_{c,b}$, $-\psi_{c,b}$)
$M_{ac,c}$ = Transformation from carriage axes to aircraft axes
– order of rotations ($-\phi_{ac,c}$, $-\theta_{ac,c}$, $-\psi_{ac,c}$)
$M_{g,ac}$ = Transformation from aircraft axes to tunnel axes
– order of rotations ($-\phi_{g,ac}$, $-\theta_{g,ac}$, $-\psi_{g,ac}$)

Transformation matrices can be combined by multiplication. For example, converting frame $\boldsymbol{F_B}$ to $\boldsymbol{F_V}$ via an intermediate frame $\boldsymbol{F_I}$ can be expressed as

$$\begin{aligned} \boldsymbol{F_V} &= M_{V,I}M_{I,B}\boldsymbol{F_B} \\ &= M_{V,B}\boldsymbol{F_B} \end{aligned} \tag{8}$$

The following transformation matrices are useful:

$$M_{g,c} = \text{Transformation from carriage axes to tunnel axes} = M_{g,ac}M_{ac,c} \tag{9}$$

$$\begin{aligned} M_{g,b} &= \text{Transformation from body axes to tunnel axes} \\ &= M_{g,ac}M_{ac,c}M_{c,b} = M_{g,c}M_{c,b} \end{aligned} \tag{10}$$

4.2 Transformation of Grid Points to Tunnel Axes

The grid points are defined in terms of a polar angle Φ_P and radial distance r, often normalised by the store diameter D to produce the non-dimensional radial calibre, r/D. The grid is defined in carriage axes in the Y_c-Z_c plane, and each point can be expressed in Cartesian coordinates with reference to carriage axes as

$$\begin{aligned} x_{c,b} &= 0 \\ y_{c,b} &= r \sin \Phi_P \\ z_{c,b} &= r \cos \Phi_P \end{aligned} \tag{11}$$

Using the transformation from carriage axes to tunnel axes, the grid points can be expressed in tunnel axes relative to carriage position as

$$\begin{pmatrix} x_{g,b} \\ y_{g,b} \\ z_{g,b} \end{pmatrix} = M_{g,c} \begin{pmatrix} x_{c,b} \\ y_{c,b} \\ z_{c,b} \end{pmatrix} \tag{12}$$

When reducing recorded tunnel data, Equations 11 and 12 can be used to calculate the grid points from tunnel axes, such that

$$\begin{pmatrix} x_{c,b} \\ y_{c,b} \\ z_{c,b} \end{pmatrix} = M^{-1}_{g,c} \begin{pmatrix} x_{g,b} \\ y_{g,b} \\ z_{g,b} \end{pmatrix} \tag{13}$$

$$\Phi_P = \arctan\left(\frac{y_{c,b}}{z_{c,b}} \right) \tag{14}$$

$$\frac{r}{D} = \frac{\sqrt{y_{c,b}^2 + z_{c,b}^2}}{D} \tag{15}$$

Most computer languages provide a function *atan2(y,x)* for evaluating the inverse tangent (arctan) with two arguments, as shown in Equation 14. This function produces angles between $-\pi$ and π. Most languages define the first argument as the numerator and the second as the denominator. Other languages including Microsoft Excel have the order of the two arguments reversed, so care should be taken during implementation.

4.3 Transformation of Store Orientations to Tunnel Axes

Store orientation angles are defined with respect to carriage axes, as required by DSTOres and STEME software. Sometimes it is desirable to express store orientation with respect to tunnel axes at each grid point. This can be found from the elements of the transformation matrix $M_{g,b}$ of Equation 10, where $M_{g,b}$, similar to Equation 7, is given by

$$M_{g,b} = \begin{bmatrix} C\theta_{g,b}C\psi_{g,b} & S\phi_{g,b}S\theta_{g,b}C\psi_{g,b} - C\phi_{g,b}S\psi_{g,b} & C\phi_{g,b}S\theta_{g,b}C\psi_{g,b} + S\phi_{g,b}S\psi_{g,b} \\ C\theta_{g,b}S\psi_{g,b} & S\phi_{g,b}S\theta_{g,b}S\psi_{g,b} + C\phi_{g,b}C\psi_{g,b} & C\phi_{g,b}S\theta_{g,b}S\psi_{g,b} - S\phi_{g,b}C\psi_{g,b} \\ -S\theta_{g,b} & S\phi_{g,b}C\theta_{g,b} & C\phi_{g,b}C\theta_{g,b} \end{bmatrix} \quad (16)$$
$$= \begin{bmatrix} M_{11} & M_{12} & M_{13} \\ M_{21} & M_{22} & M_{23} \\ M_{31} & M_{32} & M_{33} \end{bmatrix}$$

For brevity, "*C*" represents the trigonometric function cosine, and "*S*" represents sine in Equation 16. M_{ij} represents the element of the $M_{g,b}$ matrix in the i^{th} row and j^{th} column. From the elements of $M_{g,b}$ it is easy to obtain

$$\theta_{g,b} = \arcsin(-M_{31}) \quad (17)$$

$$\phi_{g,b} = \arctan\left(\frac{M_{32}}{M_{33}}\right) \quad (18)$$

$$\psi_{g,b} = \arctan\left(\frac{M_{21}}{M_{11}}\right) \quad (19)$$

These equations are valid for all $\theta_{g,b}$ $\phi_{g,b}$ and $\psi_{g,b}$ within the range specified in Equation 4.

5. Determination of Aerodynamic Loads

Aerodynamic loads at particular store positions and orientations are determined by post-processing data gathered from wind tunnel tests. This data is required for store trajectory prediction using programs such as DSTOres and STEME. Section 5.1 describes the process by which raw strain gauge balance measurements can be transformed into forces and vice versa. Sections 5.2 to 5.13 detail the full post-processing procedure used to produce the required data for store trajectory prediction. A diagram of the post-processing procedure is shown in Figure 7.

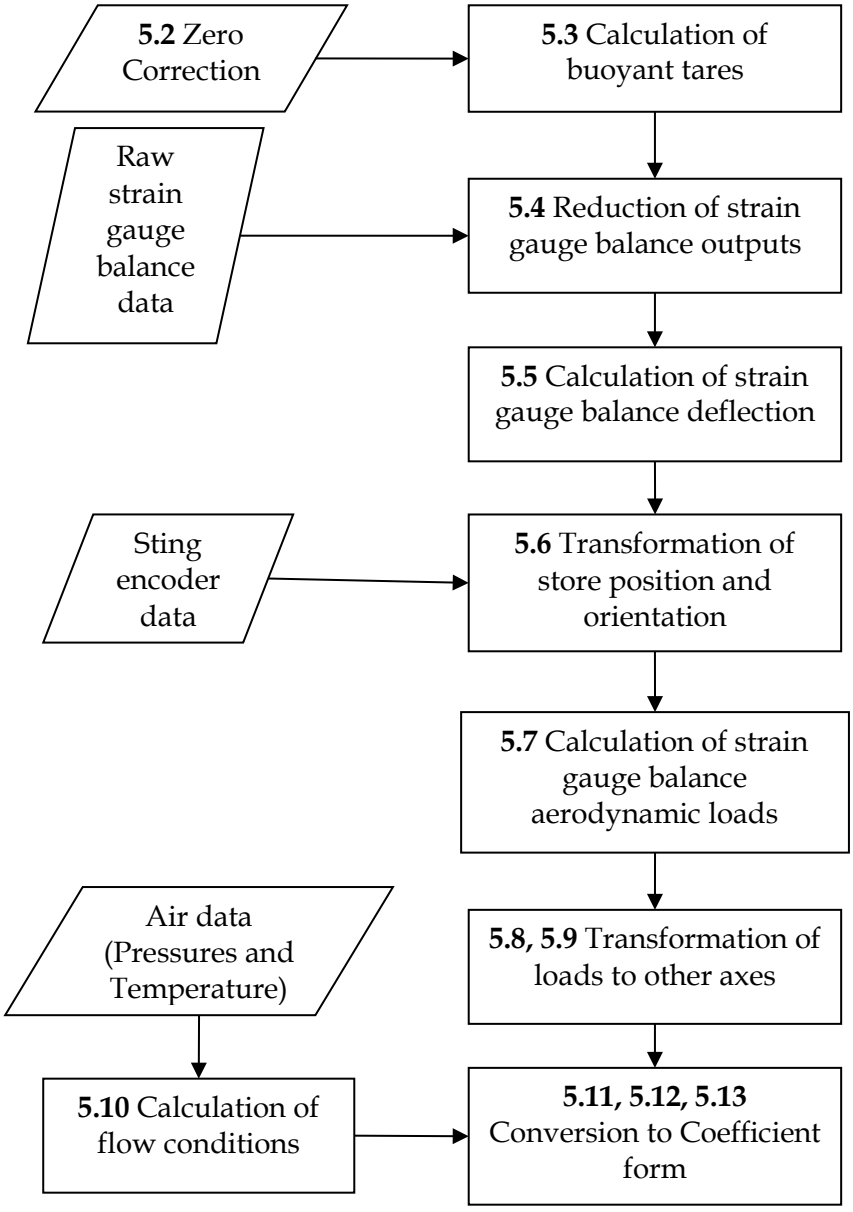

Figure 7 Post-processing procedure flow chart

5.1 Reduction of Strain Gauge Balance Outputs

Each of the output channels of a six-component strain gauge balance is represented by a 27-term second order polynomial equation of the form [8, §4.2]:

$$\left.\begin{aligned} R_i \;=\;& C_{i,1}H_1 + C_{i,2}H_2 + C_{i,3}H_3 + C_{i,4}H_4 + C_{i,5}H_5 + C_{i,6}H_6 \\ & + C_{i,11}H_1^2 + C_{i,22}H_2^2 + C_{i,33}H_3^2 + C_{i,44}H_4^2 + C_{i,55}H_5^2 + C_{i,66}H_6^2 \\ & + C_{i,12}H_1H_2 + C_{i,13}H_1H_3 + C_{i,14}H_1H_4 + C_{i,15}H_1H_5 + C_{i,16}H_1H_6 \\ & + C_{i,23}H_2H_3 + C_{i,24}H_2H_4 + C_{i,25}H_2H_5 + C_{i,26}H_2H_6 \\ & + C_{i,34}H_3H_4 + C_{i,35}H_3H_5 + C_{i,36}H_3H_6 \\ & + C_{i,45}H_4H_5 + C_{i,46}H_4H_6 \\ & + C_{i,56}H_5H_6 \end{aligned}\right\} \qquad (20)$$

$i = 1,...,6$

where the C's are the calibration coefficients and H_i are component loads.

The set of six equations represented by Equation 20 can be expressed in matrix form:

$$\boldsymbol{R} = [C1]\,\boldsymbol{H} + [C2]\,\boldsymbol{H}^* \qquad (21)$$

where

$\boldsymbol{R}$	is the vector of strain gauge balance outputs
$[C1]$	is the matrix of linear calibration coefficients
$[C2]$	is the matrix of non-linear calibration coefficients
$\boldsymbol{H}$	is the vector of component loads
$\boldsymbol{H}^*$	is the vector of squared and cross products of component loads

The calibration matrices are normalised by pre-multiplying each by a diagonal matrix $[D]$ composed of the reciprocal of the diagonal elements of $[C1]$ giving:

$$[X1] = [D]\,[C1] \qquad (22)$$

$$[X2] = [D]\,[C2]$$

Equation 21 can therefore be written as:

$$[D]\boldsymbol{R} = [D][C1]\,\boldsymbol{H} + [D][C2]\,\boldsymbol{H}^* \qquad (23)$$

or

$$\boldsymbol{H}' = [X1]\,\boldsymbol{H} + [X2]\,\boldsymbol{H}^* \qquad (24)$$

where $\boldsymbol{H}'$ is a vector of approximate component loads. Solving for $\boldsymbol{H}$ gives:

$$\boldsymbol{H} = [X1]^{-1}\,\boldsymbol{H}' - [X1]^{-1}[X2]\,\boldsymbol{H}^* \qquad (25)$$

An iterative scheme is used to determine $\boldsymbol{H}$ according to Equation 25.

A first approximation to $\boldsymbol{H}$ is obtained by ignoring the non-linear terms:

$$\boldsymbol{H_1} = [X1]^{-1}\, \boldsymbol{H'} \tag{26}$$

This is then used to obtain a first approximation to the non-linear term, Δ_1, thus:

$$\Delta_1 = [X1]^{-1}\, [X2]\, \boldsymbol{H_1}^* \tag{27}$$

where the elements of the vector $\boldsymbol{H_1}^*$ are composed of the squares and cross-product of the elements of the approximate vector $\boldsymbol{H_1}$.

A second approximation $\boldsymbol{H_2}$ is then obtained from:

$$\boldsymbol{H_2} = \boldsymbol{H_1} - \Delta_1 \tag{28}$$

The n^{th} approximation $\boldsymbol{H_n}$ is obtained iteratively by means of the generalised equations:

$$\Delta_{n-1} = [X1]^{-1}\, [X2]\, \boldsymbol{H}_{n-1}^* \tag{29}$$

$$\boldsymbol{H_n} = \boldsymbol{H_1} - \Delta_{n-1}$$

For most balances used in DSTO, the values of $\boldsymbol{H}$ typically converge to within ±0.0001 N or Nm after 2 iterations.

5.2 Zero Corrections for Strain Gauge Balance Outputs

Zero readings are taken at the beginning and end of each test run. For each zero reading, the model orientation is set to zero with respect to tunnel axes ($\psi_{g,b} = \theta_{g,b} = \phi_{g,b} = 0°$). These initial and final readings are averaged to produce the wind-off zeros, R'_{0i} ($i = 1, \cdots, 6$).

5.3 Calculation of Buoyant Tares

The tare loads applied to the strain gauge balance by the metric mass of the store model at $\theta_{g,b} = 0°$ and $\phi_{g,b} = 0°$ are computed according to the following equations [8, §4.3]:

$$\boldsymbol{H_T} = \begin{bmatrix} F_{XBALT} \\ F_{YBALT} \\ F_{ZBALT} \\ M_{XBALT} \\ M_{YBALT} \\ M_{ZBALT} \end{bmatrix} = \begin{bmatrix} -k_X \sin\theta_{g,b} \\ k_Y \cos\theta_{g,b} \sin\phi_{g,b} \\ k_Z \cos\theta_{g,b} \cos\phi_{g,b} \\ k_{MX2} \cos\theta_{g,b} \cos\phi_{g,b} - k_{MX1} \cos\theta_{g,b} \sin\phi_{g,b} \\ -k_{MY2} \sin\theta_{g,b} - k_{MY1} \cos\theta_{g,b} \cos\phi_{g,b} \\ k_{MZ2} \cos\theta_{g,b} \sin\phi_{g,b} + k_{MZ1} \sin\theta_{g,b} \end{bmatrix} \tag{30}$$

where k_X, k_Y, k_Z, k_{MX1}, k_{MX2}, k_{MY1}, k_{MY2}, k_{MZ1}, k_{MZ2} are the tare weight coefficients determined for each model configuration prior to testing.

The readings of the six strain gauge balance outputs, R_{Ti} ($i = 1, \cdots, 6$), corresponding to these loads are calculated from the strain gauge balance calibration matrices according to Equation 21.

A set of buoyant zero readings, R_{0i} ($i = 1, \cdots, 6$), are obtained by subtracting these readings from the wind-off zeros, R'_{0i} ($i = 1, \cdots, 6$), thus:

$$R_{0i} = R'_{0i} - R_{Ti} \ , \quad i = 1, \cdots, 6 \tag{31}$$

These buoyant zeros are used to correct wind-on strain gauge balance outputs.

5.4 Reduction of Strain Gauge Balance Outputs to Gross Loads

Wind-on measurements produce six raw component measurements from the strain gauge balance, (R'_i). The buoyant zeros are subtracted from these raw measurements to give absolute strain gauge balance readings, (R_i):

$$R_i = R'_i - R_{0i} \ , \qquad i = 1, \cdots, 6 \tag{32}$$

These absolute readings are converted into absolute loads according to the process described in Section 5.1. These absolute loads are termed the strain gauge balance gross loads ($\boldsymbol{H}_G$).

5.5 Calculation of Sting-Balance Deflection

Under load, the sting and strain gauge balance structure deflects. This deflection can generally be considered in combination. The deflections about the balance moment centre can be determined using the following methodology.

The components of the sting-balance deflection in balance axes are the displacements x', y', and z' and the angular deflections ν, η and χ. These are related to the applied loads, $\boldsymbol{H}_G$, by the stiffness matrix $\boldsymbol{K}$, which consists of 10 experimentally-derived coefficients, k_1, k_2, …, k_{10}:

$$\begin{bmatrix} x' \\ y' \\ z' \\ \nu \\ \eta \\ \chi \end{bmatrix} = K \cdot \boldsymbol{H}_G = \begin{bmatrix} k_{10} & 0 & 0 & 0 & 0 & 0 \\ 0 & k_8 & 0 & 0 & 0 & k_9 \\ 0 & 0 & k_6 & 0 & k_7 & 0 \\ 0 & 0 & 0 & k_1 & 0 & 0 \\ 0 & 0 & k_2 & 0 & k_3 & 0 \\ 0 & k_4 & 0 & 0 & 0 & k_5 \end{bmatrix} \begin{bmatrix} F_{XBALG} \\ F_{YBALG} \\ F_{ZBALG} \\ M_{XBALG} \\ M_{YBALG} \\ M_{ZBALG} \end{bmatrix} \tag{33}$$

5.6 Transformation of Store Position and Orientation

The model position and orientation relies on the readings from the store support (SS) system. Corrections need to be applied due to the sting-balance deflections (see Section 5.5) and any misalignment between the balance and model body axes (see Section 5.8). The store support system computes and outputs parameters in tunnel gravity axes based on feedback from angular sensors and linear displacement transducers (LDTs). The axial ($x_{g,ss}$) and vertical ($z_{g,ss}$) positions are measured by dedicated LDT's. The pitch angle pitch ($\theta_{g,ss}$) is measured by a dedicated encoder. Roll angle ($\phi_{g,ss}$) is measured by a resolver. The lateral position ($y_{g,ss}$) and yaw angle ($\psi_{g,ss}$) are calculated from the measurements of a pair of yaw encoders.

For small misalignment angles between the strain gauge balance and the model, the store support yaw, pitch, and roll offsets are nulled during initial model setup. Strain gauge balance misalignment is subsequently disregarded in the calculation of the model position and orientation. In cases where there is a large misalignment between the strain gauge balance and either the model or store support system, care must be taken to properly account for the misalignment during setup and post-processing. These cases are beyond the scope of this document.

The strain gauge balance deflection angles are not Euler angles, but as they are small they can be approximated by Euler roll, pitch and yaw angles [9, p.108], resulting in the Euler rotational transformation matrix $M_{ss,b}$, (ν, η and χ). The Euler rotational transformation matrix from the store support system orientation to tunnel gravity axes is $M_{g,ss}$, ($\phi_{g,ss}$, $\theta_{g,ss}$ and $\psi_{g,ss}$). The model position in tunnel gravity axes is given by:

$$\begin{bmatrix} x_g \\ y_g \\ z_g \end{bmatrix} = \begin{bmatrix} x_{g,ss} \\ y_{g,ss} \\ z_{g,ss} \end{bmatrix} + M_{g,ss} \begin{bmatrix} x' \\ y' \\ z' \end{bmatrix} \tag{34}$$

The model orientation with respect to tunnel gravity axes can be derived, as described in Section 4.3, from the elements of the Euler rotational transformation matrix $M_{g,b}$, which is calculated as:

$$M_{g,b} = M_{g,ss} M_{ss,b} \tag{35}$$

The location of the store model in tunnel axes relative to carriage position, ($x_{g,b}$, $y_{g,b}$, $z_{g,b}$), can be found by subtracting the carriage position in tunnel axes, ($x_{g,c}$, $y_{g,c}$, $z_{g,c}$), from the model position in tunnel axes, (x_g, y_g, z_g):

$$\begin{aligned} x_{g,b} &= x_g - x_{g,c} \\ y_{g,b} &= y_g - y_{g,c} \\ z_{g,b} &= z_g - z_{g,c} \end{aligned} \tag{36}$$

The store grid coordinates r/D and Φ_P can be calculated using Equations 13, 14 and 15.

The aircraft angle-of-attack ($\theta_{g,ac}$) is derived directly from the parent aircraft turntable encoder reading, and no data reduction is required from the raw tunnel output file. The carriage offsets ($\theta_{ac,c}$ and $\phi_{ac,c}$) are known in advance from model geometry and are not measured during testing. These angles can be used to form the rotation matrix $M_{g,c}$ (Equations 7, 9). The rotation matrix $M_{g,b}$ is calculated in Equation 35. Equation 10 can then be rearranged to get $L_{c,b}$,

$$M_{c,b} = M_{g,c}^{-1} M_{g,s} \tag{37}$$

The elements of $M_{c,b}$ can be used to calculate the store orientation angles in carriage axes ($\phi_{c,b}$, $\theta_{c,b}$ and $\psi_{c,b}$), in the same way that Equations 17, 18 and 19 are used to calculate store orientation in tunnel axes from $M_{g,b}$.

5.7 Calculation of Aerodynamic Loads in Balance Axes

The tare loads at the model attitude associated with the wind-on measurement ($\boldsymbol{H}_T$) are computed using Equation 30. Note that model attitude must be relative to tunnel axes, as calculated from the elements of the matrix $M_{g,b}$ in Equation 35 (i.e. model orientation corrected for deflections).

The aerodynamic loads in balance axes ($\boldsymbol{H}$) are then calculated by subtracting tare loads from gross loads:

$$\boldsymbol{H} = \begin{bmatrix} F_{XBAL} \\ F_{YBAL} \\ F_{ZBAL} \\ M_{XBAL} \\ M_{YBAL} \\ M_{ZBAL} \end{bmatrix} = \boldsymbol{H}_G - \boldsymbol{H}_T \tag{38}$$

5.8 Transformation of Aerodynamic Loads from Balance to Body Axes

To account for any small rotational misalignment between the balance axes and the body axes of the model, the transformation matrix used can be expressed in terms of the following offset angles:

- ξ_1 — Angle between the projection of the model X_b axis in the X_{bal}-Y_{bal} plane and the X_{bal} axis, positive nose to starboard.
- ξ_2 — Angle between the model X_b axis and its projection on the X_{bal}-Y_{bal} plane, positive nose up.
- ξ_3 — Angle between the model Z_b axis and its projection on the X_{bal}-Z_{bal} plane, positive clockwise looking forward.

Note that each of these angles rotate about the undisturbed axis, as distinct from a set of Euler angles. The rotational transformation matrix from balance axes to store body axes, derived in Appendix B.1, is given by:

$$M_{b,bal} = \begin{bmatrix} \cos\xi_1 \cos\xi_2 & \sin\xi_1 \cos\xi_2 & -\sin\xi_2 \\ \dfrac{\sin\xi_2 \sin\xi_3 - A\cos\xi_1 \sin\xi_1 \cos^2\xi_2}{B} & A & \dfrac{\cos\xi_2(\cos\xi_1 \sin\xi_3 + A\sin\xi_1 \sin\xi_2)}{B} \\ \dfrac{\cos\xi_1 \sin\xi_1 \cos^2\xi_2 \sin\xi_3 + A\sin\xi_2}{B} & -\sin\xi_3 & \dfrac{\cos\xi_2(-\sin\xi_1 \sin\xi_2 \sin\xi_3 + A\cos\xi_1)}{B} \end{bmatrix} \tag{39}$$

where

$$A = \sqrt{\cos^2 \xi_3 - \sin^2 \xi_1 \cos^2 \xi_2}$$

and

$$B = \cos^2 \xi_1 \cos^2 \xi_2 + \sin^2 \xi_2$$

The transformation of the aerodynamic forces from balance axes to body axes is therefore given by:

$$\boldsymbol{F} = M_{b,bal} \boldsymbol{F}_{\boldsymbol{BAL}} \tag{40}$$

where

$$\boldsymbol{F} = \begin{bmatrix} F_X \\ F_Y \\ F_Z \end{bmatrix} \quad \text{and} \quad \boldsymbol{F}_{\boldsymbol{BAL}} = \begin{bmatrix} F_{XBAL} \\ F_{YBAL} \\ F_{ZBAL} \end{bmatrix}$$

are the vectors of aerodynamic force in body and balance axes respectively.

To account for the translational misalignment, let (x_b, y_b, z_b) be the location of the model moment reference centre (MRC, origin of the body axes system) with respect to the balance moment centre (BMC, origin of the balance axes system). Then the transformation of the aerodynamic moments from balance axes to body axes are given by:

$$\boldsymbol{M} = M_{b,bal} \boldsymbol{M}_{\boldsymbol{BAL}} + \begin{bmatrix} 0 & z_b & -y_b \\ -z_b & 0 & x_b \\ y_b & -x_b & 0 \end{bmatrix} \boldsymbol{F} \tag{41}$$

where

$$\boldsymbol{M} = \begin{bmatrix} M_X \\ M_Y \\ M_Z \end{bmatrix}, \quad \text{and} \quad \boldsymbol{M}_{\boldsymbol{BAL}} = \begin{bmatrix} M_{XBAL} \\ M_{YBAL} \\ M_{ZBAL} \end{bmatrix}$$

are the vectors of aerodynamic moment in body and balance axes respectively.

Since the rotations are applied first, followed by translation, x_b, y_b, z_b must be measured in body axes.

5.9 Transformation to Body Axes with Origin at Centre of Gravity

For use with legacy versions of DSTOres, forces and moments must be defined about the centre of gravity (c.g.) of the real store. This will be orthogonal to the model axes system but may have its origin at a different position than the nominal MRC. To account for this translational misalignment, let (x_{cg}, y_{cg}, z_{cg}) be the location of the model c.g. with respect to the MRC. The forces applied at the c.g. do not change, and the translation of the model aerodynamic moments about the c.g. are given by:

$$\boldsymbol{M}_{c.g.} = \boldsymbol{M} + \begin{bmatrix} 0 & z_{cg} & -y_{cg} \\ -z_{cg} & 0 & x_{cg} \\ y_{cg} & -x_{cg} & 0 \end{bmatrix} \boldsymbol{F} \tag{42}$$

5.10 Calculation of Flow Conditions

The test section flow conditions are calculated from the reference transducers, settling chamber total pressure (P_t), total temperature (T_t), and plenum static pressure (P_s), using isentropic flow equations as detailed below.

5.10.1 Mach number (M)

$$M = \sqrt{\frac{2}{\gamma - 1}\left[\left(\frac{P_s}{P_t}\right)^{-\frac{\gamma-1}{\gamma}} - 1\right]} \tag{43}$$

$$= \sqrt{5\left[\left(\frac{P_s}{P_t}\right)^{-\frac{2}{7}} - 1\right]}$$

where $\gamma=1.4$ is the ratio of specific heats for air

5.10.2 Dynamic pressure (q)

$$q = \frac{\gamma}{2} P_s M^2 = 0.7 P_s M^2 \tag{44}$$

5.10.3 Reynolds number (Re)

$$Re = \frac{\rho V d}{\mu} \tag{45}$$

$$= \frac{Md}{\mu}\sqrt{\frac{\gamma}{RT_s}}\frac{P_T}{\left(1 + \frac{\gamma-1}{2}M^2\right)^{\frac{\gamma}{\gamma-1}}}$$

$$= \frac{Md}{\mu}\sqrt{\frac{1.4}{RT_s}}\frac{P_T}{\left(1 + 0.2M^2\right)^{3.5}}$$

where ρ is the flow density
V is the flow velocity
d is the model reference dimension

R is the gas constant
T_s is the static temperature (calculated from the total temperature and Mach number)
μ is the kinematic viscosity (calculated from Sutherland's law)

5.11 Conversion to Coefficient Form

The aerodynamic force coefficients, (C_X, C_Y, C_Z), and corresponding moment coefficients, (C_l, C_m, C_n), acting on the model can be calculated from the aerodynamic forces and moments in body axes:

$$C_X = \frac{F_X}{qS}; \qquad C_Y = \frac{F_Y}{qS}; \quad C_Z = \frac{F_Z}{qS}$$
$$C_l = \frac{M_X}{qSd}; \qquad C_m = \frac{M_Y}{qSd}; \quad C_n = \frac{M_Z}{qSd} \tag{46}$$

where q is the dynamic pressure, S is the model reference area, and d is the model reference dimension.

The dynamic pressure is calculated from the reference pressure transducers in accordance with Equation 44.

5.12 Transformation to Wind Axes

Aerodynamic force and moment coefficients can be converted from store body axes to wind axes using the transformation matrix:

$$M_{w,b} = \begin{bmatrix} \cos\alpha\cos\beta & \sin\beta & \sin\alpha\cos\beta \\ -\cos\alpha\sin\beta & \cos\beta & -\sin\alpha\sin\beta \\ -\sin\alpha & 0 & \cos\alpha \end{bmatrix} \tag{47}$$

The aerodynamic angles α and β are calculated using Equation 5.

5.13 Transformation to Missile Axes

Aerodynamic force and moment coefficients can be converted from store body axes to missile axes (non-rolling axes) using the transformation matrix:

$$M_{p,b} = \begin{bmatrix} 1 & 0 & 0 \\ 0 & \cos\phi_{CS} & -\sin\phi_{CS} \\ 0 & \sin\phi_{CS} & \cos\phi_{CS} \end{bmatrix} \tag{48}$$

6. Conclusion

This document has presented the algorithms required to prepare test plans for transonic wind tunnel grid testing and to reduce wind tunnel grid data for store release analysis. Elements of the procedures presented may also be amenable to other wind tunnel tests, and the algorithms have been presented in general form to assist with this. The implementation of these algorithms, while not covered in this document, is an important task that should be thoroughly verified and validated to prevent avoidable errors and uncertainty from affecting the final results. The example calculations in Appendix C can be used to validate software implementations of these algorithms.

7. References

1. US Department of Defense 1998, 'Aircraft stores compatibility: Systems engineering data requirements and test procedures', *MIL-HDBK-1763*
2. Bamber, M.J. 1966, 'Store Separation Investigations by Grid Method using Wind Tunnel Data', *Aerodynamics Laboratory Research Report 2022*, David Taylor Model Basin, Washington D.C.
3. Akroyd, G. 2001, 'Theory Base for STEME – Store Trajectory Estimation in a Matlab Environment', *Aircraft Research and Development Unit (ARDU) Report AR-1819-1 (Project I1018)*
4. Lam, S., Drobik, J., Cenko, A. 2010 'Validation of plane of symmetry testing in the DSTO transonic wind tunnel', *15th International Test and Evaluation Association (ITEA) Aircraft/Stores Compatibility Symposium*
5. The American Institute of Aeronautics and Astronautics 2012, 'Nomenclature and Axis Systems for Aerodynamic Wind Tunnel Testing', *AIAA Guide G-129-2012*
6. ASE Holdings 2003, 'User's Guide, Transonic Wind Tunnel – AMRL', *ASE/704303TP01*
7. Etkin, B. and Reid, L.D. 1996, *Dynamics of Flight: Stability and Control*, 3rd edn
8. Fairlie, B.D. 1984, 'Algorithms for the Reduction of Wind-Tunnel Data Derived from Strain Gauge Force Balances', *DSTO-ARL Aerodynamics Report ARL-AERO-R-164*
9. Mercer, C.E., Verrier, B.L., Capone, F.J., Grayston, A.M. and Sherman, C.D. 1987, 'Computations for the 16-foot Transonic Tunnel', *NASA Technical Memorandum 86319*, rev. 1

Appendix A: The DSTO Transonic Wind Tunnel

DSTO maintains and operates several experimental aerodynamic test facilities including a transonic wind tunnel (TWT). The TWT was commissioned by the US supplier, Aero Systems Engineering (ASE). It is the only facility of its kind in Australia, and enables aerodynamic research to be carried out for the Australian Defence Force (ADF). The facility operates in the transonic speed range where both viscosity and compressibility effects are important and are difficult to model using other means. This facility is a critical element of Australia's indigenous aircraft-stores combatibility clearance capability.

The TWT is a closed return-circuit continuous flow tunnel. A schematic drawing of the aerodynamic circuit and main components of the facility is shown in Figure A1. The facility has a nominal Mach number range from 0.3 to 1.2 continuously variable, and Mach 1.4 with a fixed nozzle. The total pressure can be varied from 30 kPa to 200 kPa. Flow is generated by a two-stage axial flow compressor powered by a 5.3 MW variable speed electric motor. Each stage comprises of 30 rotor blades and the fan speed can be driven to 1800 rpm. The blade positions are manually adjustable however they were fixed at predefined positions during commissioning.

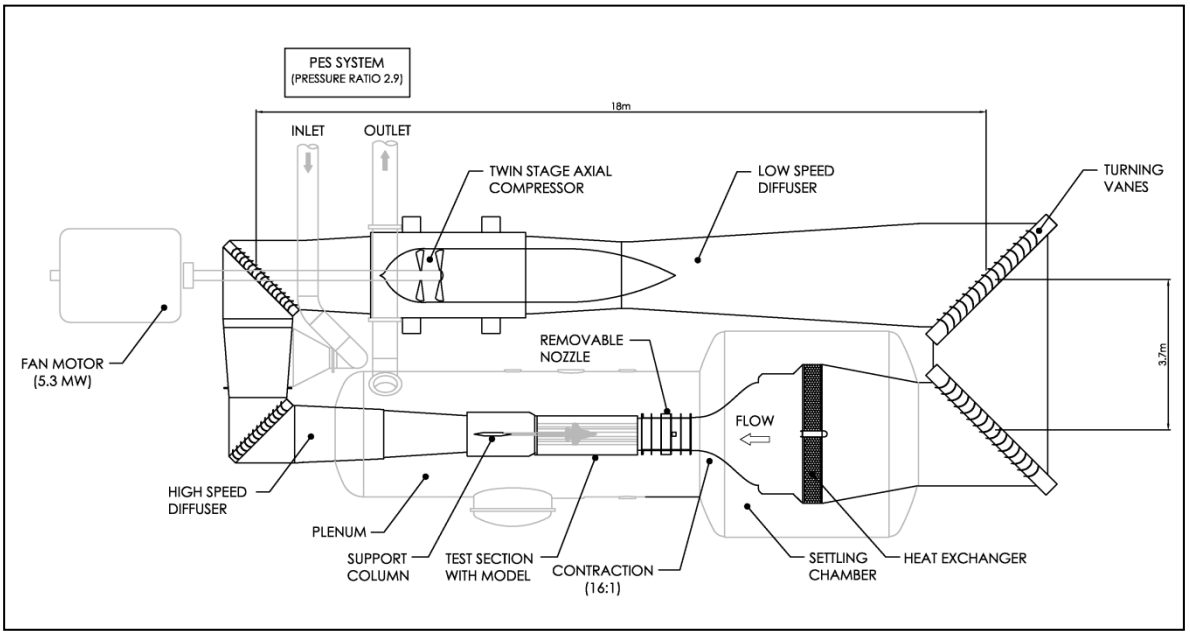

Figure A1 The DSTO transonic wind tunnel aerodynamic circuit

The tunnel is equipped with a Plenum Evacuation System (PES) to pressurise and depressurise the tunnel circuit, and to improve flow quality. The PES consists of a 17 blade centrifugal compressor driven by a 2.6 megawatt motor and operates at a constant speed of 10840 rpm. This extracts air from the plenum, compresses it by a factor of approximately 2.9 and then injects the compressed air downstream of the first corner. The effect that this has on the test section flow is equivalent to introducing a steady increase in cross-sectional area in the downstream direction.

A water-cooled heat exchanger in the settling chamber is used to control the air temperature in the test section. Turbulence conditioning screens and a 16:1 contraction provide good quality flow.

Three independent model support systems are provided:

- main model support for freestream tests of a full model, providing pitch and roll capability
- store model support to position a store model below a parent model for store release tests, with full six degree of freedom movement
- sidewall turntable model support for half-model tests, providing pitch rotation

The test section is nominally 2700 mm long and has a cross section of 806 mm square. The test section-nozzle interface is at station 3505. The test section model support interface is at station 6205. The high flow quality region extends ±400 mm from the nominal model centre at station 5257. The test section is shown in Figure A2 together with the other components which form the test leg.

The test section sidewalls are interchangeable and can be either solid or slotted. Both the top and bottom wall angles were fixed to +20 minutes each (divergent) during commissioning. However they are manually adjustable to ± 30 minutes each of arc. Each slotted wall consists of six slots per wall with a porosity of 4.97%.

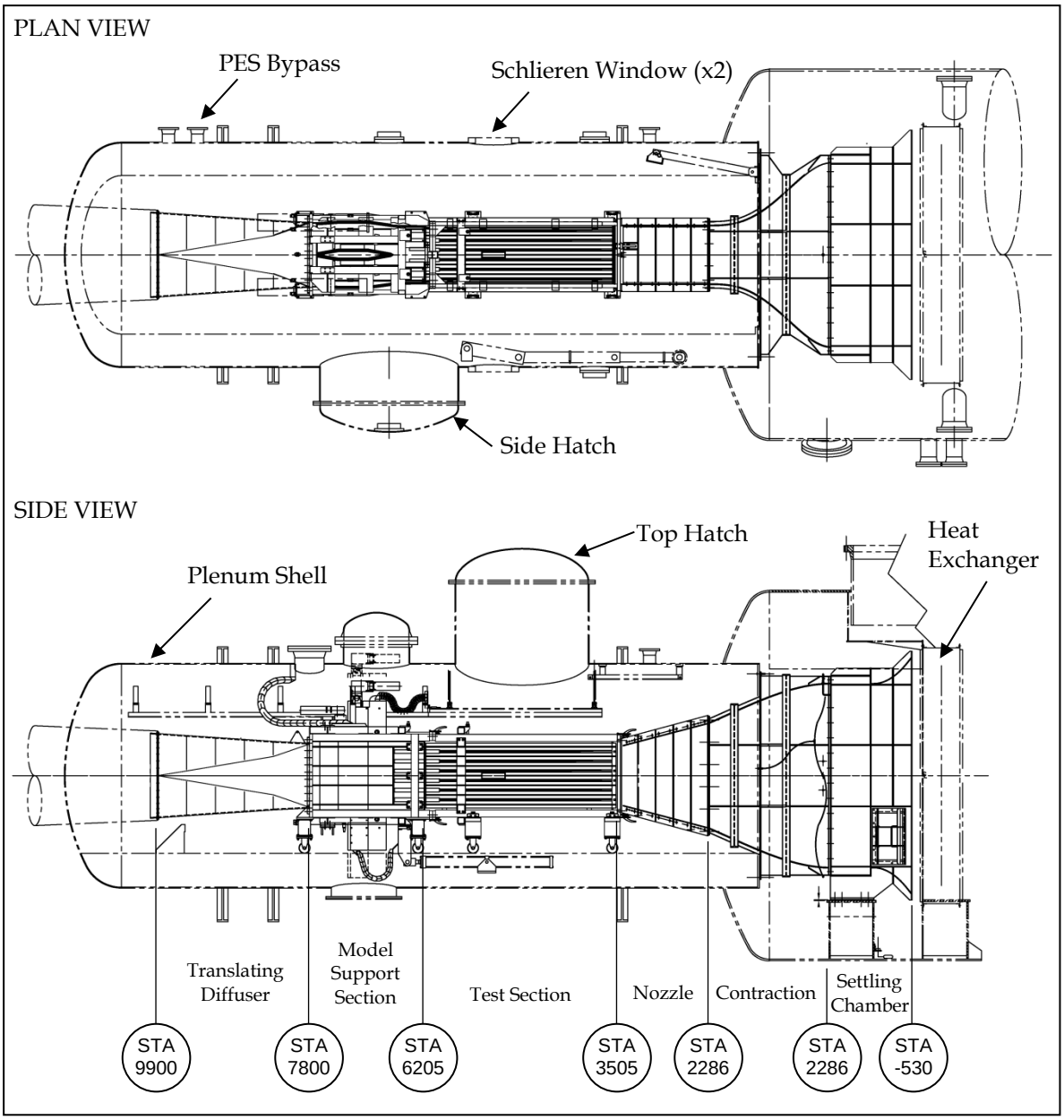

Figure A2 The DSTO transonic wind tunnel test leg and associated components

Appendix B: Transformation Derivations

B.1. Derivation of the Rotational Transformation from Balance Axes to Body Axes

The following offset angles describe the rotational misalignment between the balance axes and the body axes:

ξ_1 — Angle between the projection of the model X_b axis in the X_{bal}-Y_{bal} plane and the X_{bal} axis, positive nose to starboard

ξ_2 — Angle between the model X_b axis and its projection on the X_{bal}-Y_{bal} plane, positive nose up

ξ_3 — Angle between the model Z_b axis and its projection on the X_{bal}-Z_{bal} plane, positive clockwise looking forward

These angles are not Euler angles, but their transformation matrix can be derived by considering three Euler angle rotations:

M_1 — Rotate by ξ_1 around the model Z_b axis.

M_2 — Rotate by ξ_2 around the model Y_b axis.

M_3 — Rotate by ϕ around the model X_b axis.

$$\boldsymbol{F} = M_3(\phi)M_2(\xi_2)M_1(\xi_1)\boldsymbol{F_{BAL}} = M_{b,bal}\boldsymbol{F_{BAL}}$$

$$\begin{aligned} M_{b,bal} &= \begin{bmatrix} 1 & 0 & 0 \\ 0 & \cos\phi & \sin\phi \\ 0 & -\sin\phi & \cos\phi \end{bmatrix} \begin{bmatrix} \cos\xi_2 & 0 & -\sin\xi_2 \\ 0 & 1 & 0 \\ \sin\xi_2 & 0 & \cos\xi_2 \end{bmatrix} \begin{bmatrix} \cos\xi_1 & \sin\xi_1 & 0 \\ -\sin\xi_1 & \cos\xi_1 & 0 \\ 0 & 0 & 1 \end{bmatrix} \\ &= \begin{bmatrix} \cos\xi_1\cos\xi_2 & \sin\xi_1\cos\xi_2 & -\sin\xi_2 \\ -\sin\xi_1\cos\phi + \cos\xi_1\sin\xi_2\sin\phi & \cos\xi_1\cos\phi + \sin\xi_1\sin\xi_2\sin\phi & \cos\xi_2\sin\phi \\ \sin\xi_1\sin\phi + \cos\xi_1\sin\xi_2\cos\phi & -\cos\xi_1\sin\phi + \sin\xi_1\sin\xi_2\cos\phi & \cos\xi_2\cos\phi \end{bmatrix} \\ &= \begin{bmatrix} A_{11} & A_{12} & A_{13} \\ A_{21} & A_{22} & A_{23} \\ A_{31} & A_{32} & A_{33} \end{bmatrix} \end{aligned} \tag{B1}$$

Elements A_{11}, A_{12} and A_{13} are in terms of ξ_1 and ξ_2 only, and are therefore derived. For the rest of the elements, a relationship must now be found between ϕ and ξ_3. This can be found by considering the components of Z_b in balance axes, illustrated in Figure B1.

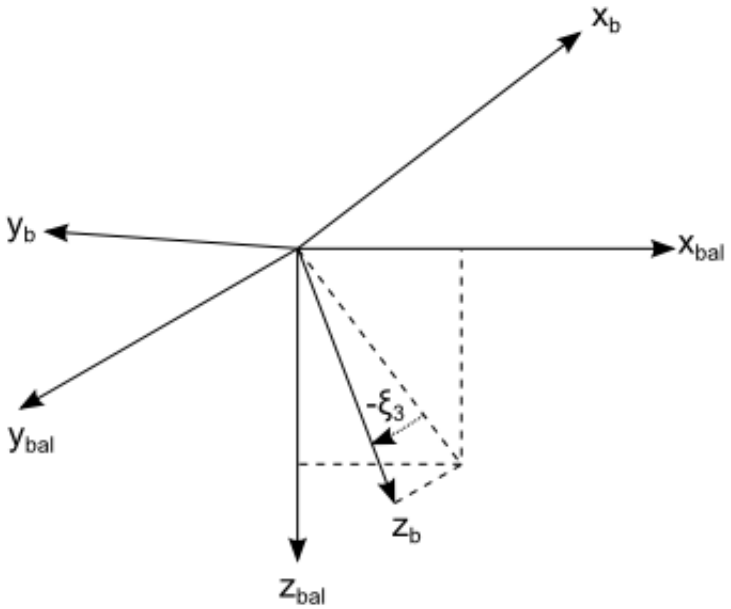

Figure B1 Components of Z_b in Balance Axes

From the Y_{bal} component, we have

$$\sin(-\xi_3) = A_{32} \tag{B2}$$
$$-\sin\xi_3 = -\cos\xi_1 \sin\phi + \sin\xi_1 \sin\xi_2 \cos\phi$$

From the projection of Z_b on the X_{bal}-Z_{bal} plane, we have

$$\cos(-\xi_3) = \sqrt{A_{31}^2 + A_{33}^2}$$
$$\cos^2\xi_3 = \left(\sin\xi_1 \sin\phi + \cos\xi_1 \sin\xi_2 \cos\phi\right)^2 + \left(\cos\xi_2 \cos\phi\right)^2$$

On expansion and rearrangement, it can be shown that

$$\cos^2\xi_3 - \sin^2\xi_1 \cos^2\xi_2 = \left(\cos\xi_1 \cos\phi + \sin\xi_1 \sin\xi_2 \sin\phi\right)^2$$

For convenience, let

$$A = \sqrt{\cos^2\xi_3 - \sin^2\xi_1 \cos^2\xi_2} = \cos\xi_1 \cos\phi + \sin\xi_1 \sin\xi_2 \sin\phi \tag{B3}$$

Hence,

$$A_{22} = \cos\xi_1 \cos\phi + \sin\xi_1 \sin\xi_2 \sin\phi = \sqrt{\cos^2\xi_3 - \sin^2\xi_1 \cos^2\xi_2} = A$$

B.1.1 Deriving A_{21}

Using Equations B2 and B3, A_{21} can be expressed in terms of ξ_1, ξ_2 and ξ_3.

$$A_{21} = -\sin\xi_1\cos\phi + \cos\xi_1\sin\xi_2\sin\phi$$
$$= \frac{\left(-\sin\xi_1\cos\phi + \cos\xi_1\sin\xi_2\sin\phi\right)\left(\cos^2\xi_1\cos^2\xi_2 + \sin^2\xi_2\right)}{\cos^2\xi_1\cos^2\xi_2 + \sin^2\xi_2}$$

Let

$$B = \cos^2\xi_1\cos^2\xi_2 + \sin^2\xi_2 \tag{B4}$$
$$A_{21}\times B = -\sin\xi_1\cos^2\xi_1\cos^2\xi_2\cos\phi - \sin\xi_1\sin^2\xi_2\cos\phi$$
$$+\cos\xi_1\sin\xi_2\cos^2\xi_1\cos^2\xi_2\sin\phi + \cos\xi_1\sin\xi_2\sin^2\xi_2\sin\phi$$
$$= \sin\xi_2\left(\cos\xi_1\sin\phi - \sin\xi_1\sin\xi_2\cos\phi\right) - \cos\xi_1\sin\xi_2\cos^2\xi_2\sin\phi$$
$$-\sin\xi_1\cos^2\xi_1\cos^2\xi_2\cos\phi + \cos\xi_1\sin\xi_2\cos^2\xi_1\cos^2\xi_2\sin\phi$$

Using Equation B2

$$A_{21}\times B = \sin\xi_2\sin\xi_3 - \cos\xi_1\sin\xi_2\cos^2\xi_2\sin\phi - \sin\xi_1\cos^2\xi_1\cos^2\xi_2\cos\phi$$
$$+\cos\xi_1\sin\xi_2\cos^2\xi_1\cos^2\xi_2\sin\phi$$
$$= \sin\xi_2\sin\xi_3 - \cos\xi_1\sin\xi_1\cos^2\xi_2\left(\sin\xi_1\sin\xi_2\sin\phi + \cos\xi_1\cos\phi\right)$$

Using Equation B3

$$A_{21} = \frac{\sin\xi_2\sin\xi_3 - A\cos\xi_1\sin\xi_1\cos^2\xi_2}{B}$$

B.1.2 Deriving A_{31}

Using Equations B2, B3 and B4, element A_{31} can be expressed in terms of ξ_1, ξ_2 and ξ_3.

$$A_{31} = \sin\xi_1\sin\phi + \cos\xi_1\sin\xi_2\cos\phi$$
$$= \frac{\left(\sin\xi_1\sin\phi + \cos\xi_1\sin\xi_2\cos\phi\right)\left(\cos^2\xi_1\cos^2\xi_2 + \sin^2\xi_2\right)}{\cos^2\xi_1\cos^2\xi_2 + \sin^2\xi_2}$$

Using Equation B4

$$A_{31}\times B = \sin\xi_1\cos^2\xi_1\cos^2\xi_2\sin\phi + \sin\xi_1\sin^2\xi_2\sin\phi$$
$$+\cos\xi_1\sin\xi_2\cos^2\xi_1\cos^2\xi_2\cos\phi + \cos\xi_1\sin\xi_2\sin^2\xi_2\cos\phi$$
$$= \cos\xi_1\sin\xi_1\cos^2\xi_2\left(\cos\xi_1\sin\phi - \sin\xi_1\sin\xi_2\cos\phi\right)$$
$$+\sin\xi_2\left(\sin\xi_1\sin\xi_2\sin\phi + \cos\xi_1\cos^2\xi_2\cos\phi + \cos\xi_1\sin^2\xi_2\cos\phi\right)$$

Using Equation B2

$$A_{31}\times B = \cos\xi_1\sin\xi_1\cos^2\xi_2\sin\xi_3$$
$$+\sin\xi_2\left(\sin\xi_1\sin\xi_2\sin\phi + \cos\xi_1\cos^2\xi_2\cos\phi + \cos\xi_1\sin^2\xi_2\cos\phi\right)$$
$$= \cos\xi_1\sin\xi_1\cos^2\xi_2\sin\xi_3 + \sin\xi_2\left(\sin\xi_1\sin\xi_2\sin\phi + \cos\xi_1\cos\phi\right)$$

Using Equation B3

$$A_{31} = \frac{\cos\xi_1 \sin\xi_1 \cos^2\xi_2 \sin\xi_3 + A\sin\xi_2}{B}$$

B.1.3 Deriving A_{23}

Using Equations B2, B3 and B4, element A_{23} can be expressed in terms of ξ_1, ξ_2 and ξ_3.

$$\begin{aligned} A_{23} &= \cos\xi_2 \sin\phi \\ &= \frac{(\cos\xi_2 \sin\phi)(\cos^2\xi_1 \cos^2\xi_2 + \sin^2\xi_2)}{\cos^2\xi_1 \cos^2\xi_2 + \sin^2\xi_2} \end{aligned}$$

Using Equation B4

$$\begin{aligned} A_{23} \times B &= \cos\xi_2 \sin\phi(\cos^2\xi_1(1-\sin^2\xi_2)+\sin^2\xi_2) \\ &= \cos\xi_2 \begin{pmatrix} \cos\xi_1(\cos\xi_1 \sin\phi - \sin\xi_1 \sin\xi_2 \cos\phi) \\ +\sin\xi_1 \sin\xi_2(\cos\xi_1 \cos\phi + \sin\xi_1 \sin\xi_2 \sin\phi) \end{pmatrix} \end{aligned}$$

Using Equations B2 and B3

$$A_{23} = \frac{\cos\xi_2(\cos\xi_1 \sin\xi_3 + A\sin\xi_1 \sin\xi_2)}{B}$$

B.1.4 Deriving A_{33}

Using Equations B2, B3 and B4, element A_{33} can be expressed in terms of ξ_1, ξ_2 and ξ_3.

$$\begin{aligned} A_{33} &= \cos\xi_2 \cos\phi \\ &= \frac{(\cos\xi_2 \cos\phi)(\cos^2\xi_1 \cos^2\xi_2 + \sin^2\xi_2)}{\cos^2\xi_1 \cos^2\xi_2 + \sin^2\xi_2} \end{aligned}$$

Using Equation B4

$$\begin{aligned} A_{33} \times B &= \cos\xi_2 \cos\phi(\cos^2\xi_1(1-\sin^2\xi_2)+\sin^2\xi_2) \\ &= \cos\xi_2 \begin{pmatrix} \cos\xi_1(\cos\xi_1 \cos\phi + \sin\xi_1 \sin\xi_2 \sin\phi) \\ -\sin\xi_1 \sin\xi_2(\cos\xi_1 \sin\phi - \sin\xi_1 \sin\xi_2 \cos\phi) \end{pmatrix} \end{aligned}$$

Using Equations B2 and B3

$$A_{33} = \frac{\cos\xi_2(-\sin\xi_1 \sin\xi_2 \sin\xi_3 + A\cos\xi_1)}{B}$$

Appendix C: Sample Calculations

The following examples are presented to show the processes required to prepare for grid testing and to reduce data from grid testing in the DSTO transonic wind tunnel. These examples can also be used to validate software developed for this purpose. Note that the numbers here are not necessarily realistic, and precision is retained for validation purposes, not as an indication of uncertainty.

C.1. Converting a Test Point to Tunnel Axes

The test point is defined inTable C1.

Table C1 Test point definition

Variable	**Symbol**	**Value**	**Units**
Store diameter	D	0.02457	m
Grid radial calibre position	r/D	3.5	ND
Grid lateral polar angle	Φ_P	-20	degrees
Parent aircraft angle-of-attack	$\theta_{g,ac}$	6	degrees
Carriage axes pitch offset	$\theta_{ac,c}$	-3	degrees
Carriage axes roll offset	$\phi_{ac,c}$	5.5	degrees
Store yaw angle (carriage axes)	$\psi_{c,b}$	5	degrees
Store pitch angle (carriage axes)	$\theta_{c,b}$	-15	degrees
Store roll angle (carriage axes)	$\phi_{c,b}$	10	degrees

C.1.1 Rotation Matrices

The rotation matrices can be calculated using Equation 7. Note that all angles not defined in Table C1 are 0. The rotation matrices are:

$$M_{g,ac} = M_2\left(-\theta_{g,ac}\right)$$

$$= \begin{bmatrix} \cos\theta_{g,ac} & 0 & \sin\theta_{g,ac} \\ 0 & 1 & 0 \\ -\sin\theta_{g,ac} & 0 & \cos\theta_{g,ac} \end{bmatrix}$$

$$= \begin{bmatrix} 0.9945219 & 0 & 0.1045285 \\ 0 & 1 & 0 \\ -0.1045285 & 0 & 0.9945219 \end{bmatrix}$$

$$M_{ac,c} = M_2(-\theta_{ac,c}).M_1(-\phi_{ac,c})$$

$$= \begin{bmatrix} \cos\theta_{ac,c} & \sin\phi_{ac,c}\sin\theta_{ac,c} & \cos\phi_{ac,c}\sin\theta_{ac,c} \\ 0 & \cos\phi_{ac,c} & -\sin\phi_{ac,c} \\ -\sin\theta_{ac,c} & \sin\phi_{ac,c}\cos\theta_{ac,c} & \cos\phi_{ac,c}\cos\theta_{ac,c} \end{bmatrix}$$

$$= \begin{bmatrix} 0.9986295 & -0.0050162 & -0.0520950 \\ 0 & 0.9953962 & -0.0958458 \\ 0.0523360 & 0.0957144 & 0.9940320 \end{bmatrix}$$

$$M_{c,b} = M_3(-\psi_{c,b}).M_2(-\theta_{c,b}).M_1(-\phi_{c,b})$$

$$= \begin{bmatrix} \cos\theta_{c,b}\cos\psi_{c,b} & \sin\phi_{c,b}\sin\theta_{c,b}\cos\psi_{c,b} - \cos\phi_{c,b}\sin\psi_{c,b} \\ \cos\theta_{c,b}\sin\psi_{c,b} & \sin\phi_{c,b}\sin\theta_{c,b}\sin\psi_{c,b} + \cos\phi_{c,b}\cos\psi_{c,b} \\ -\sin\theta_{c,b} & \sin\phi_{c,b}\cos\theta_{c,b} \end{bmatrix}$$

$$\begin{matrix} \cos\phi_{c,b}\sin\theta_{c,b}\cos\psi_{c,b} + \sin\phi_{c,b}\sin\psi_{c,b} \\ \cos\phi_{c,b}\sin\theta_{c,b}\sin\psi_{c,b} - \sin\phi_{c,b}\cos\psi_{c,b} \\ \cos\phi_{c,b}\cos\theta_{c,b} \end{matrix} \Bigg]$$

$$= \begin{bmatrix} 0.9622502 & -0.1306041 & -0.2387826 \\ 0.0841860 & 0.9771432 & -0.1952023 \\ 0.2588190 & 0.1677313 & 0.9512513 \end{bmatrix}$$

$$M_{g,c} = M_{g,ac}M_{ac,c}$$

$$= \begin{bmatrix} 0.9986295 & 0.0050162 & 0.0520950 \\ 0 & 0.9953962 & -0.0958458 \\ -0.0523360 & 0.0957144 & 0.9940320 \end{bmatrix}$$

$$M_{g,b} = M_{g,ac}M_{ac,c}M_{c,b} = M_{g,c}M_{c,b}$$

$$= \begin{bmatrix} 0.9748369 & -0.1167856 & -0.1898791 \\ 0.0589917 & 0.9565683 & -0.2854770 \\ 0.2149719 & 0.2670922 & 0.9393874 \end{bmatrix}$$

C.1.2 Grid Position in Tunnel Axes

The grid position in carriage axes is:

$$\begin{aligned} x_{c,b} &= 0 \text{ m} \\ y_{c,b} &= r \sin \Phi_P \\ &= \text{-}0.0294120 \text{ m} \\ z_{c,b} &= r \cos \Phi_P \\ &= 0.0808089 \text{ m} \end{aligned}$$

where $r = r/D*D = 0.085995$ m.

The grid position in tunnel axes is calculated as follows:

$$\begin{pmatrix} x_{g,b} \\ y_{g,b} \\ z_{g,b} \end{pmatrix} = M_{g,c} \begin{pmatrix} x_{c,b} \\ y_{c,b} \\ z_{c,b} \end{pmatrix}$$

$$= \begin{pmatrix} 0.0040622 \\ \text{-}0.0370218 \\ 0.0775114 \end{pmatrix} \text{m}$$

C.1.3 Store Orientation in Tunnel Axes

The store orientation in tunnel axes is found from the elements of $M_{g,b}$ in accordance with Equations 17, 18 and 19:

$$M_{g,b}(3,1) = -\sin \theta_{g,b} = 0.2149719$$

$$\theta_{g,b} = -12.4139°$$

$$M_{g,b}(3,2) = \sin \phi_{g,b} \cos \theta_{g,b} = 0.2670922$$

$$M_{g,b}(3,3) = \cos \phi_{g,b} \cos \theta_{g,b} = 0.9393874$$

$$\phi_{g,b} = \arctan\left(\frac{M_{g,b}(3,2)}{M_{g,b}(3,3)} \right)$$

$$= 15.8718°$$

$$M_{g,b}(1,1) = \cos \theta_{g,b} \cos \psi_{g,b} = 0.9748369$$

$$M_{g,b}(2,1) = \cos \theta_{g,b} \sin \psi_{g,b} = 0.0589917$$

$$\psi_{g,b} = \arctan\left(\frac{M_{g,b}(2,1)}{M_{g,b}(1,1)} \right)$$

$$= 3.4630°$$

C.2. Data Reduction for a Test Point Measurement

The general test data for this example are listed in Table C2, strain gauge balance coefficients are listed in Table C3, and data specific to this particular test point are listed in Table C4. Strain gauge balance calibration data is given in Equations C1 and C2.

Table C2 Example test data

Variable	Symbol	Value	Units
Store diameter	D	0.02457	m
Store reference area	S_{ref}	0.000474	m²
Location of MRC w.r.t BMC	$\boldsymbol{s}_{MRC,BMC}$	[-0.0025, 0, 0]	m
Zero pitch reading, averaged	θ_0	0.00206301998705	degrees
Zero roll reading, averaged	ϕ_0	0.010111324	degrees
Gross strain gauge balance zero readings, averaged	$\boldsymbol{R'_0}$	[0, 0.000180001294, 0.000769806525, 0.000359504257, -0.000335901155, 0.000030521535]	mV/V

Table C3 Strain gauge balance coefficients

Coefficient	Value	Units
Deflection coefficients		
k_1	1.4689	degrees/Nm
k_2	-0.0144	degrees/N
k_3	0.4378	degrees/Nm
k_4	0.01447	degrees/N
k_5	0.4515	degrees/Nm
k_6	0.03295	mm/N
k_7	-0.2403	mm/Nm
Tare coefficients		
k_X	0	N
k_Y	3.7399786	N
k_Z	3.7844698	N
k_{MX1}	0.0084307101	Nm
k_{MX2}	0.00020851234	Nm
k_{MY1}	0.00038854941	Nm
k_{MY2}	0.0095461681	Nm
k_{MZ1}	0.00022903467	Nm
k_{MZ2}	0.00016170646	Nm

Table C4 Test point specific example data

Variable	Symbol	Value	Units
Gross strain gauge balance readings	$\boldsymbol{R}'$	[0, -0.1400, 0.5400, 0.1200, 0.3500, 0.0800]	mV/V
Parent aircraft angle-of-attack	$\theta_{g,ac}$	4.99	degrees
Carriage axes pitch offset	$\theta_{ac,c}$	-3	degrees
Carriage axes roll offset	$\phi_{ac,c}$	5.5	degrees
Absolute model position, from store support feedback	$[x_{g,ss}, y_{g,ss}, z_{g,ss}]$	[6.838, -109.636, 175.804]	mm
Relative model position, from store support feedback	$[xr_{g,ss}, yr_{g,ss}, zr_{g,ss}]$	[3.642, -37.926, 103.808]	mm
Model orientation in tunnel axes, from store support feedback	$[\phi_{g,ss}, \theta_{g,ss}, \psi_{g,ss}]$	[-5.004, -8.500, 0.010]	degrees
Tunnel static pressure	P_S	75.04	kPa
Tunnel total pressure	P_T	126.91	kPa
Tunnel total temperature	T_T	308.502	degrees Kelvin

$$[X1] = \begin{bmatrix} 1 & 0 & 0 & 0 & 0 \\ 0 & 1.34957955824748E-02 & 1.85872010975616E-04 & 9.10153188177356E-05 & 5.5107087643103E-05 \\ 0 & -2.01270863980661E-04 & 1.33297098851551E-02 & 1.41126499894741E-04 & 3.06594432331226E-05 \\ 0 & -2.92097108131194E-03 & 1.2276290588619E-03 & 2.49931437883246 & -9.29033874774701E-05 \\ 0 & -7.31078706779773E-04 & 4.85721196061138E-03 & 1.06194111329936E-03 & 0.545184191413662 \\ 0 & -3.78793090574685E-03 & 6.00071467638071E-04 & 3.62245421958098E-03 & -1.56855750759619E-02 \end{bmatrix} \begin{matrix} 0 \\ -1.33844648392573E-04 \\ -1.32195338917485E-04 \\ -1.32284773603211E-03 \\ 1.57455876867475E-03 \\ 0.546663837059006 \end{matrix} \quad \text{(C1)}$$

$$[D] = \begin{bmatrix} 1 & 0 & 0 & 0 & 0 & 0 \\ 0 & 1 & 0 & 0 & 0 & 0 \\ 0 & 0 & 1 & 0 & 0 & 0 \\ 0 & 0 & 0 & 1 & 0 & 0 \\ 0 & 0 & 0 & 0 & 1 & 0 \\ 0 & 0 & 0 & 0 & 0 & 1 \end{bmatrix} \quad \text{(C2)}$$

C.2.1 Buoyant Tares

Buoyant tares are calculated from the averaged zero readings taken at the start and end of the run:

$$\begin{aligned} F_{XBALT} &= -k_X \sin\theta_0 \\ &= 0 \\ F_{YBALT} &= k_Y \cos\theta_0 \sin\phi_0 \\ &= 0.000660016068866 \\ F_{ZBALT} &= k_Z \cos\theta_0 \cos\phi_0 \\ &= 3.784469738615505 \\ M_{XBALT} &= k_{MX2} \cos\theta_0 \cos\phi_0 - k_{MX1} \cos\theta_0 \sin\phi_0 \\ &= 0.000207024519512 \\ M_{YBALT} &= -k_{MY2} \sin\theta_0 - k_{MY1} \cos\theta_0 \cos\phi_0 \\ &= -0.000388893127716 \\ M_{ZBALT} &= k_{MZ2} \cos\theta_0 \sin\phi_0 + k_{MZ1} \sin\theta_0 \\ &= 0.000000036784027 \end{aligned}$$

The equivalent voltage for these forces and moments is calculated and subtracted from the gross strain gauge zero readings to give the buoyant zero readings ($\boldsymbol{R_0}$). Note that the strain gauge balance calibration equation is simplified due to the first order calibration being used.

$$\boldsymbol{H_{T0}} = \begin{bmatrix} F_{XBALT} \\ F_{YBALT} \\ F_{ZBALT} \\ M_{XBALT} \\ M_{YBALT} \\ M_{ZBALT} \end{bmatrix}$$

$$\boldsymbol{R_T} = [D]^{-1}[X1]\boldsymbol{H_{T0}}$$

$$= \begin{bmatrix} 0 \\ -0.000753116592538 \\ 0.050444371598445 \\ 0.001051155549775 \\ -0.000095972088956 \\ -0.000501243687842 \end{bmatrix}$$

$$\boldsymbol{R_0} = \boldsymbol{R_0'} - \boldsymbol{R_T}$$

$$= \begin{bmatrix} 0 \\ 0.000933117886538 \\ -0.049674565073445 \\ -0.000691651292775 \\ -0.000239929066044 \\ 0.000531765222842 \end{bmatrix}$$

C.2.2 Gross Aerodynamic Loads

For each test point, the strain gauge balance readings are corrected for buoyant tares. The gross aerodynamic loads are then calculated from these readings:

$$\boldsymbol{R} = \boldsymbol{R'} - \boldsymbol{R_0}$$

$$= \begin{bmatrix} 0 \\ -0.140933117886538 \\ 0.589674565073445 \\ 0.120691651292775 \\ 0.350239929066044 \\ 0.079468234777158 \end{bmatrix}$$

$$\boldsymbol{H_G} = [X1]^{-1}[D]\boldsymbol{R}$$

$$= \begin{bmatrix} 0 \\ -9.697177517617988 \\ 44.126648133526913 \\ 0.045657007450587 \\ 0.645302229378291 \\ 0.151917836927412 \end{bmatrix}$$

C.2.3 Sting-Balance Deflections

Deflections of the sting-balance assembly are calculated using gross loads:

$$\begin{bmatrix} x' \\ y' \\ z' \\ \nu \\ \eta \\ \chi \end{bmatrix} = \begin{bmatrix} k_{10} & 0 & 0 & 0 & 0 & 0 \\ 0 & k_8 & 0 & 0 & 0 & k_9 \\ 0 & 0 & k_6 & 0 & k_7 & 0 \\ 0 & 0 & 0 & k_1 & 0 & 0 \\ 0 & 0 & k_2 & 0 & k_3 & 0 \\ 0 & k_4 & 0 & 0 & 0 & k_5 \end{bmatrix} \boldsymbol{H}_G$$

$$= \begin{bmatrix} 0 \\ 0 \\ 1.298906930280108 \\ 0.067065578244168 \\ -0.352910417100972 \\ -0.071727255307206 \end{bmatrix}$$

C.2.4 Store Model Position and Orientation

Store model position and orientation is measured by the store support system transducers. Positions and orientations are output in tunnel axes referenced both to the tunnel coordinate system origin ("absolute") and to a user specified location ("relative"), which in this case is the carriage position. Model orientations and both absolute and relative positions are corrected for sting-balance deflections. Model orientations and relative positions are then transformed into carriage axes, and the radial distance and polar angle are calculated.

The following Euler rotational transformation matrices are required:

$$M_{g,ss} = M_3(-\psi_{g,ss}) M_2(-\theta_{g,ss}) M_1(-\phi_{g,ss})$$

$$= \begin{bmatrix} \cos\theta_{g,ss}\cos\psi_{g,ss} & \sin\phi_{g,ss}\sin\theta_{g,ss}\cos\psi_{g,ss} - \cos\phi_{g,ss}\sin\psi_{g,ss} \\ \cos\theta_{g,ss}\sin\psi_{g,ss} & \sin\phi_{g,ss}\sin\theta_{g,ss}\sin\psi_{g,ss} + \cos\phi_{g,ss}\cos\psi_{g,ss} \\ -\sin\theta_{g,ss} & \sin\phi_{g,ss}\cos\theta_{g,ss} \end{bmatrix}$$

$$\begin{bmatrix} \cos\phi_{g,ss}\sin\theta_{g,ss}\cos\psi_{g,ss} + \sin\phi_{g,ss}\sin\psi_{g,ss} \\ \cos\phi_{g,ss}\sin\theta_{g,ss}\sin\psi_{g,ss} - \sin\phi_{g,ss}\cos\psi_{g,ss} \\ \cos\phi_{g,ss}\cos\theta_{g,ss} \end{bmatrix}$$

$$= \begin{bmatrix} 0.9852463 & 0.0871996 & -0.1472613 \\ -0.0862672 & 0.9961908 & 0.0127189 \\ 0.1478094 & 0.0001726 & 0.9890158 \end{bmatrix}$$

$$M_{ss,b} = M_3(-\chi).M_2(-\eta).M_1(-\nu)$$

$$= \begin{bmatrix} \cos\eta\cos\chi & \sin\nu\sin\eta\cos\chi - \cos\nu\sin\chi & \cos\nu\sin\eta\cos\chi + \sin\nu\sin\chi \\ \cos\eta\sin\chi & \sin\nu\sin\eta\sin\chi + \cos\nu\cos\chi & \cos\nu\sin\eta\sin\chi - \sin\nu\cos\chi \\ -\sin\eta & \sin\nu\cos\eta & \cos\nu\cos\eta \end{bmatrix}$$

$$= \begin{bmatrix} 0.9999802 & 0.0012447 & -0.0061609 \\ -0.0012519 & 0.9999985 & -0.0011628 \\ 0.0061594 & 0.0011705 & 0.9999803 \end{bmatrix}$$

$$M_{g,b} = M_{g,ss} M_{ss,b}$$

$$= \begin{bmatrix} 0.9852463 & 0.0871996 & -0.1472613 \\ -0.0862672 & 0.9961908 & 0.0127189 \\ 0.1478094 & 0.0001726 & 0.9890158 \end{bmatrix} \begin{bmatrix} 0.9999802 & 0.0012447 & -0.0061609 \\ -0.0012519 & 0.9999985 & -0.0011628 \\ 0.0061594 & 0.0011705 & 0.9999803 \end{bmatrix}$$

$$= \begin{bmatrix} 0.9842107 & 0.0882534 & -0.1534297 \\ -0.0874342 & 0.9960969 & 0.0120917 \\ 0.1538980 & 0.0015142 & 0.9880856 \end{bmatrix}$$

$$M_{g,ac} = M_2(-\theta_{g,ac})$$

$$= \begin{bmatrix} \cos\theta_{g,ac} & 0 & \sin\theta_{g,ac} \\ 0 & 1 & 0 \\ -\sin\theta_{g,ac} & 0 & \cos\theta_{g,ac} \end{bmatrix}$$

$$= \begin{bmatrix} 0.9945219 & 0 & 0.1045285 \\ 0 & 1 & 0 \\ -0.1045285 & 0 & 0.9945219 \end{bmatrix}$$

$$M_{ac,c} = M_2(-\theta_{ac,c}).M_1(-\phi_{ac,c})$$

$$= \begin{bmatrix} \cos\theta_{ac,c} & \sin\phi_{ac,c}\sin\theta_{ac,c} & \cos\phi_{ac,c}\sin\theta_{ac,c} \\ 0 & \cos\phi_{ac,c} & -\sin\phi_{ac,c} \\ -\sin\theta_{ac,c} & \sin\phi_{ac,c}\cos\theta_{ac,c} & \cos\phi_{ac,c}\cos\theta_{ac,c} \end{bmatrix}$$

$$= \begin{bmatrix} 0.9986295 & -0.0050162 & -0.0520950 \\ 0 & 0.9953962 & -0.0958458 \\ 0.0523360 & 0.0957144 & 0.9940320 \end{bmatrix}$$

$$M_{g,c} = M_{g,ac} M_{ac,c}$$

$$= \begin{bmatrix} 0.9993969 & 0.0033283 & 0.0345652 \\ 0 & 0.9953962 & -0.0958458 \\ -0.0347251 & 0.0957879 & 0.9947959 \end{bmatrix}$$

$$M_{g,b} = M_{g,ac} M_{ac,c} M_{c,b} = M_{g,c} M_{c,b}$$

$$M_{c,b} = M_{\mathrm{g,c}}^{-1} M_{g,b}$$

$$= \begin{bmatrix} 0.9782730 & 0.0881476 & -0.18764861 \\ -0.0690144 & 0.9919498 & 0.1061721 \\ 0.1954968 & -0.0909148 & 0.9764812 \end{bmatrix}$$

Store model position is calculated by transforming strain gauge balance deflections into tunnel axes and adding them to store support system encoder feedback:

$$\begin{bmatrix} x_{g,b} \\ y_{g,b} \\ z_{g,b} \end{bmatrix} = \begin{bmatrix} x_{g,ss} \\ y_{g,ss} \\ z_{g,ss} \end{bmatrix} + M_{g,ss} \begin{bmatrix} x' \\ y' \\ z' \end{bmatrix}$$

$$= \begin{bmatrix} 6.646721 \\ 109.619479 \\ 177.088640 \end{bmatrix}$$

$$\begin{bmatrix} xr_{g,b} \\ yr_{g,b} \\ zr_{g,b} \end{bmatrix} = \begin{bmatrix} xr_{g,ss} \\ yr_{g,ss} \\ zr_{g,ss} \end{bmatrix} + M_{g,ss} \begin{bmatrix} x' \\ y' \\ z' \end{bmatrix}$$

$$= \begin{bmatrix} 3.450721 \\ -37.909479 \\ 105.092640 \end{bmatrix}$$

Store model orientations in tunnel axes are found from the elements of $M_{g,b}$:

$$M_{g,b}(3,1) = -\sin\theta_{g,b} = 0.1538980$$

$$\theta_{g,b} = -8.8529°$$

$$M_{g,b}(3,2) = \sin\phi_{g,b} \cos\theta_{g,b} = 0.0015142$$

$$M_{g,b}(3,3) = \cos\phi_{g,b} \cos\theta_{g,b} = 0.9880856$$

$$\phi_{g,b} = \arctan\left(\frac{M_{g,b}(3,2)}{M_{g,b}(3,3)}\right)$$

$$= 0.0878°$$

$$M_{g,b}(1,1) = \cos\theta_{g,b}\cos\psi_{g,b} = 0.9842107$$
$$M_{g,b}(2,1) = \cos\theta_{g,b}\sin\psi_{g,b} = -0.0874342$$
$$\psi_{g,b} = \arctan\left(\frac{M_{g,b}(2,1)}{M_{g,b}(1,1)}\right)$$
$$= 5.0767°$$

Likewise, store model orientations in carriage axes are found from the elements of $M_{c,b}$:

$$M_{c,b}(3,1) = -\sin\theta_{c,b} = 0.1954968$$
$$\theta_{c,b} = -11.2737°$$
$$M_{c,b}(3,2) = \sin\phi_{c,b}\cos\theta_{c,b} = -0.0909148$$
$$M_{c,b}(3,3) = \cos\phi_{c,b}\cos\theta_{c,b} = 0.9764812$$
$$\phi_{c,b} = \arctan\left(\frac{M_{c,b}(3,2)}{M_{c,b}(3,3)}\right)$$
$$= -5.3192°$$

$$M_{c,b}(1,1) = \cos\theta_{c,b}\cos\psi_{c,b} = 0.9782730$$
$$M_{c,b}(2,1) = \cos\theta_{c,b}\sin\psi_{c,b} = -0.0690144$$
$$\psi_{c,b} = \arctan\left(\frac{M_{c,b}(2,1)}{M_{c,b}(1,1)}\right)$$
$$= -4.0354°$$

Model positions in carriage axes, relative to carriage position, are:

$$\begin{bmatrix} xr_{c,b} \\ yr_{c,b} \\ zr_{c,b} \end{bmatrix} = M_{g,c}^{-1}\begin{bmatrix} xr_{g,b} \\ yr_{g,b} \\ zr_{g,b} \end{bmatrix}$$
$$= \begin{bmatrix} -0.200709 \\ -27.656858 \\ 108.298462 \end{bmatrix}$$

The grid radial calibre position and lateral polar angle can then be calculated. Care should be taken that $yr_{c,b}$, $zr_{c,b}$ and D all have consistent units. In the following calculation, mm are used.

$$r/D = \frac{\sqrt{yr_{c,b}^2 + zr_{c,b}^2}}{D}$$
$$= 4.5492$$

$$\Phi_P = \arctan\left(\frac{yr_{c,b}}{zr_{c,b}}\right)$$
$$= -14.3258°$$

C.2.5 Aerodynamic Loads in Balance Axes

The corrected store model orientations are used to calculate wind-on metric mass tare loads, which are then subtracted from gross loads to give aerodynamic loads in balance axes:

$$\begin{aligned}
F_{XBALT} &= -k_X \sin\theta_{g,b} \\
&= 0 \\
F_{YBALT} &= k_Y \cos\theta_{g,b} \sin\phi_{g,b} \\
&= 0.00566317 \\
F_{ZBALT} &= k_Z \cos\theta_{g,b} \cos\phi_{g,b} \\
&= 3.73938002 \\
M_{XBALT} &= k_{MX2} \cos\theta_{g,b} \cos\phi_{g,b} - k_{MX1} \cos\theta_{g,b} \sin\phi_{g,b} \\
&= 0.00019326 \\
M_{YBALT} &= -k_{MY2} \sin\theta_{g,b} - k_{MY1} \cos\theta_{g,b} \cos\phi_{g,b} \\
&= 0.00108522 \\
M_{ZBALT} &= k_{MZ2} \cos\theta_{g,b} \sin\phi_{g,b} + k_{MZ1} \sin\theta_{g,b} \\
&= -0.00003500
\end{aligned}$$

$$\boldsymbol{H_T} = \begin{bmatrix} F_{XBALT} \\ F_{YBALT} \\ F_{ZBALT} \\ M_{XBALT} \\ M_{YBALT} \\ M_{ZBALT} \end{bmatrix}$$

$$\boldsymbol{H} = \boldsymbol{H_G} - \boldsymbol{H_T}$$

$$= \begin{bmatrix} 0 \\ -9.70284069 \\ 40.38726811 \\ 0.04546375 \\ 0.64421701 \\ 0.15195284 \end{bmatrix}$$

C.2.6 Aerodynamic Loads in Body Axes

Rotational misalignment between the balance and body axes is represented by the non-Euler transformation matrix $M_{b,bal}$. In most cases, any small offset will be nulled during initial model setup. If there is a large misalignment, care must be taken to properly account for the misalignment at various stages in this process. This case is beyond the scope of this document. In this example there is no misalignment, so the transformation matrix is the 3-dimensional identity matrix,

$$M_{b,bal} = \begin{bmatrix} 1 & 0 & 0 \\ 0 & 1 & 0 \\ 0 & 0 & 1 \end{bmatrix}$$

The origin of the store body axes, the Model Moment Reference Centre (MRC), is displaced from the origin of the balance axes, the Balance Moment Centre (BMC) by the vector $\boldsymbol{s}_{MRC,BMC}$. The aerodynamic loads about the store body axes, $\boldsymbol{F}$ and $\boldsymbol{M}$, can be calculated from the aerodynamic loads about the balance axes, $\boldsymbol{F}_{BAL}$ and $\boldsymbol{M}_{BAL}$, as follows:

$$\boldsymbol{F}_{BAL} = \boldsymbol{H}(i = 1,2,3)$$

$$\boldsymbol{M}_{BAL} = \boldsymbol{H}(i = 4,5,6)$$

$$\boldsymbol{F} = M_{b,bal}\boldsymbol{F}_{BAL}$$

$$= \begin{bmatrix} 0 \\ -9.70284069 \\ 40.38726811 \end{bmatrix}$$

$$\boldsymbol{s}_{MRP,BMC} = \begin{bmatrix} x_b \\ y_b \\ z_b \end{bmatrix} = \begin{bmatrix} -0.0025 \\ 0 \\ 0 \end{bmatrix}$$

$$\boldsymbol{M} = L_{SBAL}\boldsymbol{M}_{BAL} + \begin{bmatrix} 0 & z_b & -y_b \\ -z_b & 0 & x_b \\ y_b & -x_b & 0 \end{bmatrix}\boldsymbol{F}$$

$$= \begin{bmatrix} 0.04546375 \\ 0.54324884 \\ 0.12769574 \end{bmatrix}$$

Note that when translating the moments, the forces in store body axes are used. The displacement vector should therefore be in store body axes. Any deflection between the BMC and MRC is accommodated during balance calibration, and it is assumed that the assembly is rigid between the metric end of the balance and the MRC.

C.2.7 Tunnel Flow Conditions

Tunnel Mach number is calculated as:

$$M = \sqrt{\frac{2}{\gamma - 1}\left[\left(\frac{P_s}{P_t}\right)^{-\frac{\gamma-1}{\gamma}} - 1\right]}$$
$$= 0.90$$

Dynamic pressure is calculated as:

$$q = \frac{\gamma}{2} P_s M^2$$
$$= 42.544 \text{ kPa}$$

Reynolds number is not used for further results in this example, and is not calculated here.

C.2.8 Aerodynamic Force and Moment Coefficients

The aerodynamic loads in body axes are used to calculate body force and moment coefficients.

$$C_X = \frac{F_X}{qS} = 0$$

$$C_Y = \frac{F_Y}{qS} = -0.4812$$

$$C_Z = \frac{F_Z}{qS} = 2.0028$$

$$C_l = \frac{M_X}{qSd} = 0.0918$$

$$C_m = \frac{M_Y}{qSd} = 1.0964$$

$$C_n = \frac{M_Z}{qSd} = 0.2577$$

The body force and moment coefficients can be transformed into missile axes, or non-rolling axes, using the Euler rotational transformation matrix:

$$M_{p,b} = \begin{bmatrix} 1 & 0 & 0 \\ 0 & \cos\phi_{c,b} & -\sin\phi_{c,b} \\ 0 & \sin\phi_{c,b} & \cos\phi_{c,b} \end{bmatrix}$$

$$\begin{bmatrix} C_{Xp} \\ C_{Yp} \\ C_{Zp} \end{bmatrix} = M_{p,b} \begin{bmatrix} C_X \\ C_Y \\ C_Z \end{bmatrix}$$
$$= \begin{bmatrix} 0 \\ -0.2934 \\ 2.0387 \end{bmatrix}$$

$$\begin{bmatrix} C_{lp} \\ C_{mp} \\ C_{np} \end{bmatrix} = M_{p,b} \begin{bmatrix} C_l \\ C_m \\ C_n \end{bmatrix}$$
$$= \begin{bmatrix} 0.0918 \\ 1.1156 \\ 0.1550 \end{bmatrix}$$

DEFENCE SCIENCE AND TECHNOLOGY ORGANISATION
DOCUMENT CONTROL DATA

1. DLM/CAVEAT (OF DOCUMENT)

2. TITLE

Data Reduction Algorithms for Store Separation Grid Testing

3. SECURITY CLASSIFICATION (FOR UNCLASSIFIED REPORTS THAT ARE LIMITED RELEASE USE (L) NEXT TO DOCUMENT CLASSIFICATION)

Document	(U)
Title	(U)
Abstract	(U)

4. AUTHOR(S)

Jonathan Dansie and Adam Blandford

5. CORPORATE AUTHOR

DSTO Defence Science and Technology Organisation
506 Lorimer St
Fishermans Bend Victoria 3207 Australia

6a. DSTO NUMBER	6b. AR NUMBER	6c. TYPE OF REPORT	7. DOCUMENT DATE
DSTO-TN-1339	AR-016-054	Technical Note	August 2014

8. FILE NUMBER	9. TASK NUMBER	10. TASK SPONSOR	11. NO. OF PAGES	12. NO. OF REFERENCES
2013/1181253	AIR 07/321	AOSG	45	9

13. DSTO Publications Repository

http://dspace.dsto.defence.gov.au/dspace/

14. RELEASE AUTHORITY

Chief, Aerospace Division

15. SECONDARY RELEASE STATEMENT OF THIS DOCUMENT

Approved for public release

OVERSEAS ENQUIRIES OUTSIDE STATED LIMITATIONS SHOULD BE REFERRED THROUGH DOCUMENT EXCHANGE, PO BOX 1500, EDINBURGH, SA 5111

16. DELIBERATE ANNOUNCEMENT

No Limitations

17. CITATION IN OTHER DOCUMENTS Yes

18. DSTO RESEARCH LIBRARY THESAURUS

Wind tunnels, Wind tunnel tests, Algorithms, Data processing, Instrumentation, Data reduction, Strain gauges, Calibration, Computer programs, Load tests, Stores clearance, Aerodynamics

19. ABSTRACT

Store separation testing is undertaken to ensure that stores can be safely released from aircraft in flight. Grid testing in wind tunnels produces data that can be used to predict store separation behaviour. This document describes the algorithms used to prepare test plans for store separation grid testing and to reduce grid data to the form required for analysis. The information is presented in a general form, and may also provide a useful reference for other forms of wind tunnel testing.